

Voltage Stability Analysis of Grid-Connected Wind Farms with FACTS Devices

Hamza Ahmad M. Isied

Submitted to the
Institute of Graduate Studies and Research
in partial fulfillment of the requirements for the degree of

Master of Science
in
Electrical and Electronic Engineering

Eastern Mediterranean University
July 2022
Gazimağusa, North Cyprus

Approval of the Institute of Graduate Studies and Research

Prof. Dr. Ali Hakan Ulusoy
Director

I certify that this thesis satisfies all the requirements as a thesis for the degree of Master of Science in Electrical and Electronic Engineering.

Assoc. Prof. Dr. Rasime Uygurođlu
Chair, Department of Electrical and
Electronic Engineering

We certify that we have read this thesis and that in our opinion it is fully adequate in scope and quality as a thesis for the degree of Master of Science in Electrical and Electronic Engineering.

Assoc. Prof. Dr. Reza Sirjani
Supervisor

Examining Committee

1. Prof. Dr. Osman K krcr

2. Assoc. Prof. Dr. Reza Sirjani

3. Asst. Prof. Dr. Moein Jazayeri

ABSTRACT

The renewable energy resources are the key for our future since the fossil fuel is limited and has very dangerous effects in the environment. However, the rapid growth in the usage of renewable-based generation poses challenges for the power system operators. In this thesis, a systematic approach will be proposed for voltage stability analysis of a power system with grid-connected wind farms using various techniques. Static analysis is used to analyze the voltage stability of the system under study, whilst the dynamic analysis is used to evaluate the voltage magnitude fluctuation during time. The static techniques that have been used are Power Flow, P–V curve analysis, and Q–V modal analysis. In addition, different FACTS devices such as Static Var Compensator (SVC) and Static Synchronous Compensator (STATCOM) are added to the system as reactive power compensators, considering improving the violated voltage magnitudes of the weak buses.

An IEEE-14 bus test system is used in order to study the voltage stability analysis on and the effects of implement FACTS devices such as STATCOM and SVC on the power system, where the voltage stability analysis have been done in 8 different cases showing the weakest areas and buses in the system as well as placing these different FACTS devices at once in different weak buses in order to show the effects of these devices in the voltage stability analysis outputs. The last case shows the optimal solution of the test power system where both FACTS devices STATCOM and SVC have been used showing that the system becomes more stable, and the voltage magnitude profile is enhanced in the whole power system as well as the laudability of the system increased.

Keywords: wind farm, voltage stability analysis, static analysis, dynamic analysis, FACTS devices, STATCOM, SVC.

ÖZ

Fosil yakıtların sınırlı olması ve çevreye çok tehlikeli etkileri olması nedeniyle yenilenebilir enerji kaynakları geleceğimizin anahtarıdır. Bununla birlikte, yenilenebilir bazlı üretimin kullanımındaki hızlı büyüme, güç sistemi operatörleri için zorluklar ortaya çıkarmaktadır. Bu tezde, çeşitli teknikler kullanılarak şebekeye bağlı rüzgar santrallerine sahip bir güç sisteminin gerilim kararlılık analizi için sistematik bir yaklaşım önerilecektir. Statik analiz, incelenen sistemin voltaj kararlılığını analiz etmek için kullanılırken, dinamik analiz, zaman içindeki voltaj büyüklüğü dalgalanmasını değerlendirmek için kullanılır. Kullanılan statik teknikler, Güç Akışı, P-V eğrisi analizi ve Q-V modal analizidir. Ayrıca Statik Var Kompansatör (SVC) ve Statik Senkron Kompansatör (STATCOM) gibi farklı FACTS cihazları, zayıf baraların ihlal edilen gerilim büyüklüklerinin iyileştirilmesi düşünülerek reaktif güç kompanzatorü olarak sisteme eklenmiştir.

STATCOM ve SVC gibi uygulama FACTS cihazlarının güç sistemi üzerindeki voltaj kararlılık analizini ve etkilerini incelemek için bir IEEE-14 bus test sistemi kullanıldı. Gerilim kararlılık analizi, sistemdeki en zayıf alanları ve baraları gösteren 8 farklı durumda ve bu farklı FACTS cihazlarının farklı zayıf baralara bir kerede yerleştirilmesi ile bu cihazların voltaj stabilite analiz çıktılarındaki etkilerini göstermek için yapılmıştır. Son durum, hem STATCOM hem de SVC FACTS cihazlarının kullanıldığı test güç sisteminin optimal çözümünü göstermektedir. Sistemin daha kararlı hale geldiğini ve tüm güç sisteminde voltaj büyüklüğü profilinin arttığını ve ayrıca sistemin takdir edilebilirliğinin arttığını gösterir.

Anahtar Kelimeler: rüzgar çiftliđi, voltaj kararlılık analizi, statik analiz, dinamik analiz, FACTS cihazları, STATCOM, SVC.

ACKNOWLEDGEMENT

I would like to thank Assoc. Prof. Dr. Reza SIRJANI for his supervision, assistance, and guidance from the very beginning of this thesis, as well as for providing me with incredible experiences throughout the process. Above all, and most importantly, he constantly encouraged and supported me in many ways. His thoughts, experiences, and ambitions have enriched and motivated my development as a student. I owe him far more than he realizes.

I would like to thank the members of my graduate committee, especially Prof. Dr. Osman KÜKRER and Asst. Prof. Dr. Moein JAZAYERI, for their advice and guidance. I am appreciative in every manner for all of their suggestions and encouragement.

I would also like to express my gratitude to my family, my dad Ahmad Isied, my mom Ameera Baidas, my brother Mahmoud Isied and my sisters for their endless support, help and encouragement for me, as well as I would like to thank my friends Faisal Mustafa, Omar Abu Nabaa, Arian Tabrizi and Saman Kanzi for their moral support, understanding and encouragement.

To all who are not mentioned but in one way or another helped in completion of this study, thank you very much.

TABLE OF CONTENTS

ABSTRACT	iii
ÖZ	v
ACKNOWLEDGEMENT	vii
LIST OF TABLES	x
LIST OF FIGURES	xi
1 INTRODUCTION	1
1.1 Background	1
1.2 Problem Statement	2
1.3 The Objectives of the Research.....	3
1.4 Thesis Organization.....	3
2 LITERATURE REVIEW.....	5
2.1 Literature Review	5
3 METHODOLOGY.....	15
3.1 Voltage Stability Analysis Techniques	15
3.1.1 Power Flow.....	15
3.1.2 Q-V Sensitivity	18
3.1.3 P-V Curve.....	20
3.1.4 Dynamic Analysis	21
3.2 FACTS Devices.....	22
3.2.1 STATCOM Device.....	22
3.2.2 SVC Device	23
3.3 FACTS Devices Placement Method	24
3.4 Wind Farm Modeling.....	25

3.5 PSAT Software.....	27
4 RESULT AND DISCUSSION	29
4.1 Case Study (IEEE 14- Bus Test System)	29
4.2 Voltage Stability Analysis.....	30
4.2.1 Voltage Stability Analysis for Power System without FACTS (Case 1) ..	30
4.2.2 Voltage Stability Analysis for Power System with STATCOM at Bus 14 (Case 2).....	34
4.2.3 Voltage Stability Analysis for Power System with STATCOM at Bus 9 (Case 3)	37
4.2.4 Voltage Stability Analysis for Power System with STATCOM at Bus 4 (Case 4)	40
4.2.5 Voltage Stability Analysis for Power System with SVC at Bus 14 (Case 5).....	43
4.2.6 Voltage Stability Analysis for Power System with SVC at Bus 9 (Case 6)	46
4.2.7 Voltage Stability Analysis for Power System with SVC at Bus 4 (Case 7)	49
4.2.8 Voltage Stability Analysis for Power System with SVC at Bus 9 and STATCOM at Bus 14 (Case 8)	52
4.2.9 Dynamic Analysis of the System	55
4.3 Comparison Between This Work and Past Works	58
5 CONCLUSION	59
REFERENCES.....	61

LIST OF TABLES

Table 4.1: Two ranges of voltage levels, depending on ANSI C84.1.....	30
Table 4.2: Power flow result without compensator.	31
Table 4.3: Q-V model analysis without compensator.....	32
Table 4.4: Power flow result with STATCOM on bus 14.	35
Table 4.5: Q-V model analysis result with STATCOM on bus 14.....	36
Table 4.6: Power flow result with STATCOM on bus 9.	38
Table 4.7: Q-V model analysis result with STATCOM on bus 9.....	39
Table 4.8: Power flow result with STATCOM on bus 4.	41
Table 4.9: Q-V model analysis result with STATCOM on bus 4.....	42
Table 4.10: Power flow result with SVC on bus 14.....	44
Table 4.11: Q-V model analysis result with SVC on bus 14.	45
Table 4.12: Power flow result with SVC on bus 9.....	47
Table 4.13: Q-V model analysis result with SVC on bus 9.	48
Table 4.14: Power flow result with SVC on bus 4.....	50
Table 4.15: Q-V model analysis result with SVC on bus 4.	51
Table 4.16: Power flow result with SVC on bus 9 and STATCOM on bus 14.	53
Table 4.17: Q-V model analysis result with SVC on bus 9 and STATCOM on bus 14.	54

LIST OF FIGURES

Figure 3.1: P-V curve analysis.....	21
Figure 3.2: SATCOM model.....	23
Figure 3.3: SVC model.	24
Figure 3.4: Flow chart for placement method.....	25
Figure 3.5: DFIG equipped wind turbine diagram.....	26
Figure 3.6: Main page of PSAT.	27
Figure 3.7: PSAT plot page.....	28
Figure 4.1: IEEE 14 bus test system.....	29
Figure 4.2: P-V curve for voltage at bus 1-bus 5	33
Figure 4.3: P-V curve for voltage at bus 6-bus 10	33
Figure 4.4: P-V curve for voltage at bus 11-bus 14	34
Figure 4.5: P-V curve after compensation for voltage at bus 1-bus 5.....	36
Figure 4.6: P-V curve after compensation for voltage at bus 6-bus 10.....	37
Figure 4.7: P-V curve after compensation for voltage at bus 11-bus 14.....	37
Figure 4.8: P-V curve after compensation for voltage at bus 1-bus 5.....	39
Figure 4.9: P-V curve after compensation for voltage at bus 6-bus 10.....	40
Figure 4.10: P-V curve after compensation for voltage at bus 11-bus 14	40
Figure 4.11: P-V curve after compensation for voltage at bus 1-bus 5	42
Figure 4.12: P-V curve after compensation for voltage at bus 6-bus 10	43
Figure 4.13: P-V curve after compensation for voltage at bus 11-bus 14	43
Figure 4.14: P-V curve after compensation for voltage at bus 1-bus 5	45
Figure 4.15: P-V curve after compensation for voltage at bus 6-bus 10	46
Figure 4.16: P-V curve after compensation for voltage at bus 11-bus 14	46

Figure 4.17: P-V curve after compensation for voltage at bus 1-bus 5	48
Figure 4.18: P-V curve after compensation for voltage at bus 6-bus 10	49
Figure 4.19: P-V curve after compensation for voltage at bus 11-bus 14	49
Figure 4.20: P-V curve after compensation for voltage at bus 1-bus 5	51
Figure 4.21: P-V curve after compensation for voltage at bus 6-bus 10	52
Figure 4.22: P-V curve after compensation for voltage at bus 11-bus 14	52
Figure 4.23: P-V curve after compensation for voltage at bus 1-bus 5	54
Figure 4.24: P-V curve after compensation for voltage at bus 6-bus 10	55
Figure 4.25: P-V curve after compensation for voltage at bus 11-bus 14	55
Figure 4.26: Time domain before compensation for voltage at bus 1-bus5.....	56
Figure 4.27: Time domain before compensation for voltage at bus 6-bus 10.....	56
Figure 4.28: Time domain before compensation for voltage at bus 10-bus14.....	56
Figure 4.29: Time domain after compensation for voltage at bus 1-bus5	57
Figure 4.30: Time domain after compensation for voltage at bus 6-bus10	57
Figure 4.31: Time domain after compensation for voltage at bus 11-bus14	58

Chapter 1

INTRODUCTION

1.1 Background

The need of the energy increase every day while the world is developing and the limitation of the fossil fuel make the world concern about the future as well as the greenhouse gases generated from the usage of fossil fuel affect the environment and destroy our planet earth, until the renewable energy sources have been discovered and used as energy sources that have no harm in the environment and the planet earth, these resources such as solar and wind is the main focus of the countries because of the unlimited free resources as well as using these sources is not effecting the environment because these resources have no greenhouses associated with them when they operate [1]. The increment of renewable energy sources usage comes with challenges such as dependence on the location, variability, voltage and system stability and power quality [2]. Voltage and system stability is one of the most important concerns since it is still a huge problem with blackout occur on the system, such as the blackout happened in the power system in 2012 effected almost 670 million person in India, and the blackout happened in the power system in 2014 effected almost 20 million person in Egypt [3].

Voltage collapse or blackout are the events that affect the stability of voltage in the system causing a very low voltage in the power system network. Where ability of keeping all the system buses voltages constant after being affected by a disturbance is refer to the voltage stability, the system stability improvement express in how faster

the system is in clearing and acting when a disturbance affect the system. Voltage stability analysis refers to a set of calculation and assessment done for the system in order to determine the unstable and the weakest areas that can cause a blackout and system instability in the power system, voltage stability analysis contain two main analysis sections, first one is the static analysis which includes the power flow study, P-V curves and the Q-V sensitivity, the second section is the dynamic analysis where the voltage magnitude calculated during simulation time.

Flexible Alternating Current Transmission System (known as FACTS) devices are power electronic devices implemented on the power system to absorb or generate active and reactive power in the weakest area in the system in order to enhance the voltage profile for the power system. Static Var Compensator (SVC) and Static Synchronous Compensator (STATCOM) are the two FACTS devices that are used in this thesis for improving the system stability. SVC is the first generation of FACTS devices family, before a three decades ago this technology was invented by the institute of electric power research (EPRI), around 800 SVC device was invented and implemented across the world for both industrial and utility application, the first ever implementation of the SVC device in the power system was in 1974 [4].

1.2 Problem Statement

The increment in usage of the renewable energy resources came with challenges expressed in the following points:

- 1- Intermittency, this means when the power system generation is not continuously available because of different uncontrolled external factors.
- 2- Variability, this means when the power source fluctuates and produces energy not depending on the demand, and it can be classified in two sections, firstly is

the predictable variability such as the day cycle, and secondly is the unpredictable variability such as unsure weather forecast.

- 3- Partial controllability, this means when the system is not totally controlled and that comes because of uncontrolled external factors.
- 4- Location dependency, this means the importance of the power system location in terms of the most hours of sunshine and high wind speed.

1.3 The Objectives of the Research

Objectives of the research can be addressed in four points that have been achieved in this study:

- 1- To study the stability of the power system and determine the weakest areas by implementing the voltage stability analysis technique.
- 2- To create a systematic approach for the engineers to follow in network planning, including static analysis such as power flow, P-V curve, and Q-V sensitivity, while the dynamic analysis shows the voltage magnitude fluctuation during the time domain simulation.
- 3- To make the system more reliable and more controllable and prevent the system from blackout or instability in case of load increment or fault happening in the power system.
- 4- To show a comparison between both FACTS devices STATCOM and SVC by implementing each one of them in the system and performing the voltage stability analysis.

1.4 Thesis Organization

Five chapters are organized in this thesis as follows:

Chapter 1: Shows an introduction which includes the study background and the problem statement of this topic followed by the thesis organization.

Chapter 2: Shows the literature review of the works and articles that have been done before in this topic include performing voltage stability analysis on a certain power system and the use of the FACTS devices in order to enhance the power system stability and improve the voltage profile in certain power system.

Chapter 3: Shows a detailed explanation of the study methodology, and explanation of the FACTS devices STATCOM and SVC that are used in this thesis as well as wind farm model explanation is addressed in this chapter.

Chapter 4: Shows the result and discussion part after performing the methodology study in the power system for 8 different cases, includes finding the weakest area in the system and implement different FACTS devices in these areas separately and report the result with explanation.

Chapter 5: Shows recommendation and conclusion of the thesis.

Chapter 2

LITERATURE REVIEW

2.1 Literature Review

The literature review of this study shows that FACTS devices can be used to achieve perfect voltage stability. Moreover, FACTS devices are widely used to fix the voltage instability problems with a large share of PV and wind energy.

Bakola et al. in [5] have shown voltage stability analysis including firstly static analysis such as PV, QV curves and power flow has been used to test the system and voltage stability, secondly dynamic analysis used to show the performance of the power system components. The output shows that both SVC and STATCOM can be used in order to develop the load ability and voltage stability of the system and also to develop the power transmit capability of the transmission lines [5].

Sai et al. in [6] have shown the control of the power transmission system by using FACTS devices. By minimizing the power loss of the system and considering the voltage collapse, the optimal placement and sizing of FACTS devices is found and calculated. United power flow controller (UPFC) and the interline power flow controller (IPFC) are the FACTS devices that are used in the system. To calculate the power flow of the transmission system they used Newton-Raphson (NR) method. As a result the system voltage is stable and satisfies the requirement as they simulated in MATLAB program.

Sidnei et al. in [7] have shown the optimal placement of the FACTS devices by using the evolutionary algorithm that aims to enhance the stability of voltage. The output data results showed that voltage of the IEEE test system is more stable, and showed that EA-based method performed better than the other methods. EA also performed better than other methods in the simulation goal function depending on voltage deviation.

Samo et al. in [8] have shown the importance of FACTS devices on the stability of voltage depending on calculating the PV curves. The methodology is explained theoretically by using an in-depth approach. The approach is presented in this paper for different FACTS devices such as STATCOM and SVC which depend on a deep calculation of the area between the PV curves and the voltage range of PV. It presents detailed explanation of how suitable the different FACTS devices for keeping the voltage stable in the system without forgetting the difference between device parameters.

Priti et al. in [9] have shown the effect of different FACTS devices to maintain the stability of voltage in P-Q plane by using the load flow result which is obtained by using Newton-Raphson method and impedance matrix and also to find the optimal place for the different FACTS devices such as STATCOM and SVC where it can work in the most useful and efficient way to reach the most enhanced and improved voltage stability margin. They used the MATLAB program to simulate their result and the effectiveness of different FACTS devices.

Samo et al. in [10] have shown that the different FACTS devices such as a Controllable Series Compensator (CSC) have a significant impact and effect on the stability of

voltage in the power system. It shows the control of the voltage stability by using mathematical derivation depending on CSC and a Static Synchronous Series Compensator (SSSC) to maintain the stability of voltage in a simulated IEEE 5-bus system to prove the new analytical equations. Also showed that every different FACTS device has its own parameters and its own advantages, and if the system was low voltage it's proven that the SSSC is better than CSC.

Priti et al. in [11] have shown a 3-D diagram of P-Q-V space that is obtained by using Thevenin equivalent to show the voltage stability enhancement and improvement after adding the FACTS devices. The diagram with the result provided by using the MATLAB program clarifies the impact and effect of different FACTS devices. By using the AVSR and index L the best placement place for FACTS devices is found and the voltage and line stability analysis is done and compared with each other in order to determine the weakest bus in the system or line, which considers the optimal place in order to place the FACTS there. It is performed on IEEE-14 and IEEE-30 test systems. Where the outputs show the enhancement in the system voltage stability.

Sai et al. in [12] have shown the best settings for different FACTS devices and calculated the optimal place for FACTS and its parameters by using particle swarm optimization technique and adaptive gravitational search technique. By using the power loss of the system and the rating of voltage collapse the best optimal place for different FACTS devices are found. It is also shown that the power flow of the system is obtained by using Newton-Raphson technique for the load flow, and a simulated IEEE-30 bus system is done using MATLAB program to test the improvement and enhancement of the voltage profile.

Abdelaziz et al. in [13] used the STATCOM device in order to enhance the system voltage stability and decrease the voltage drop and remove the blackout of the transmission system by using the efficient voltage regulation method. Simulation output showed the improvement and the enhancement of the voltage and the efficacy of STATCOM in improving the system quality.

Abdelnasser et al. in [14] used the two control units, firstly fuzzy-IP and secondly fuzzy-PID used with one of the FACTS devices which is (D-STATCOM) in order to enhance the power quality of the system and enhance the voltage stability of an AC-DC micro grid system. These fuzzy algorithms can improve the dynamic performance which improve the quality of the system and give it more sleeking stable signal.

Shiva et al. in [15] used the practical swarm optimization in order to find the optimal place for in the power system to implement one of the FACTS devices which is SVC in order to increase the system liability and security. They calculate the effectiveness of the FACTS device in every line outage and differentiate the rustle of using the FACTS device SVC with the result of not using the device which shows the enhancement of the system after adding the SVC device.

Sudhanshu et al. in [16] used the interconnected hybrid power system (IHPS) as a system to analyze the voltage stability and the frequency enhancement and control for a sample micro grid. It evaluated the system response on different operating conditions to find the following IHPS in the existence of FACTS devices such as (STATCOM), as well as, enhance in the voltage magnitude and the stability of the power system as result of implementing the control frequency technique.

A voltage stability analysis for wind power systems is done in Ref [5]. It shows the impacts of rising the penetration in the wind power system, and Voltage stability borders found by using PV analysis. Fixable AC transmission system devices are implemented and have an effective enhancement and improvement on power indemnification technique and improvement in voltage profile.

Biplab et al. in [17] have shown the functional coordination of FACTS devices by using the swarm intelligent technique. A sample test system of IEEE-50 sample system and IEEE-30 sample system is used. They showed that using FACTS devices along with reactive power planning gives a more enhanced result of PV planner and even in the cost of operating the system.

Ramin et al. in [18] have shown the control of voltage being done by using a FACTS device such as SVC and showed that after the fault happens the fluctuation of reactive power has been decreased and the changes of voltage being controlled. In the control block diagram SVC clarify the voltage profile as the reference along with voltage variation. By using a MATLAB program the system powered by wind energy is being simulated under different situations such as adding or removing the FACTS devices. The output shows what SVC is capable of in improving the stability of voltage and solving the voltage variation and fluctuation.

Ping et al. in [19] have shown that FACTS devices such as STATCOM has a big role in the stability of voltage and the power system in the transmission network these devices parameters has been calculated by using the inelegant optimization technique. The authors used the combination of particle swarm algorithm and the genetic algorithm which give us the intelligent optimization technique. The efficiency of

keeping the voltage in control and suppressing low frequency power oscillation is the purpose of using STATCOM. Output has shown that a simulated IEEE-4 bus system and IEEE-16 bus system got improved and enhanced control in power and voltage after adding the STATCOM device.

Chi et al. in [20] used FACTS devices such as STATCOM on a transmission power system in order to improve the voltage regulation and get a better share of loads. A d-q frame impedances boundaries are found by this device and showed that voltage regulation was the main purpose of the fluctuation of the power system. Also, the number of different FACTS devices used in the system and the placement of them was the main factor to reach stability. A two STATCOM are implemented in the power system grid to reach the aim of stability of power system and voltage.

Shenlong et al. in [21] revealed that the use of a novel dynamic state estimation scheme, along with the STATCOM control scheme, can reduce the voltage instability of a fuel cell power station that is connected to a complex power grid. That control scheme, which is compared with two other methods, exhibited superior performance in reducing the voltage flickers and deviations. The study also aims to analyze the effects of STATCOM on the electrical system's voltage oscillations caused by electrical faults. The power system is stable during the analysis after implementing the control technique. The internal dynamic states of the system are obtained through the use of the UKF algorithm.

Li et al. in [22] used the FACTS devices in order to improve and enhance the stability of the power system. The phase compensation technique is used with STATCOM in order to remove the low frequency fluctuation. Simulated power systems show the

enhancement and improvement in the stability after implementing the STATCOM device on the integrated wind farm power system on a different disturbance circumstances.

Gajendra et al. in [23] have shown a review of FACTS devices controlled by an adaptive technique in order to stabilize the power system and improve its quality for a grid with renewable energy penetration. After implementing these algorithms the performance and the hardware experiment to show the impacts of these algorithms is reported.

Shenglong et al. in [24] simulated a complex power system to control the voltage and the frequency on it by using the sliding mode control technique. By using one of the FATS devices such as SVC the frequency of the load regulation is achieved. The authors implemented the sliding mode control that is easy to perform and a good performance in improving the stability of system voltages and regulating frequencies.

Yacine et al. in [25] have shown the improvement of voltage stability as an effect of using the fixed capacitor thyristor filter compensator. And they also visualize the effect of voltage stability in preventing the system from voltage collapse or blackout. Stability of voltage is reached after designing and implementing the FC-TCR and model it by closed loop control algorithm. The power system is simulated by using the MATLAB program and ensured that the following design played a big role in improving the stability of voltage and enhancing the power quality of the power system.

Mehrdad et al. in [26] solved the optimization problem by using the bee colony

algorithm as well as improved the system stability by finding the best optimal place to place the FACTS devices in the power system. Finding the optimal place for FACTS devices is done in high accuracy and at a good convergence speed using the bee colony algorithm. A comparison is done between two algorithms, the bee colony algorithm and the genetic algorithm and the simulated system result shows that the bee colony is more efficient algorithm compared with the genetic algorithm.

Faruk et al. in [27] used the MCDM algorithm in order to find the optimal placement of FACTS devices in the power system such as SVC. The system is simulated and tested by using a PSAT toolbox powered by MATLAB program, IEEE-14-30-118 bus test systems are performed in the program and by using the analytic hierarchy process and the MCDN technique the optimal place on these system are found in order to improve the reliability of the system and the consistency of it, as well as the analyzing of the effects of the phase shifting transformer along with the overloaded lines.

Srivats et al. in [28] have shown a way to enhance the stability of voltage and improve the rotor angle by using the hierarchical decentralized control planner. By using some measurement such as synchro phasor measurement to activate the control agent in order to find the losing rotor angle and the instability of voltage of the system. Rotor angle stability along with voltage stability being reached using FACTS devices controlled by Lyapunov algorithm. If the voltage fluctuation happens in the system due to a different situation such as fault, the secondary voltage control agent gets the control action after it gets the data that was provided from the tertiary voltage control agent. The result of a simulated IEEE-118 bus power sample system shows that the efficiency of FACTS devices and hierarchical decentralized control method is high in improving the voltage stability and rotor angle.

Hamidreza et al. in [29] have shown the improvement in the distribution of the power system quality by adding the unified power quality conditioner, as well as digital implantation are known as the controller and the discrete model are performed together. And to get the best stabilizer of the grid system the Hamilton Jacobi grid stabilizer is being used in the system. UPQC is used in the system and proved that it can enhance the quality of power system and increase the quality of distribution in the RN system, and showed that the grid's stability is increased and increases the power conditioning tasks by using the UPQC series voltage. The stability of the grid inverter along with the synchronous generator is being reached by the minimum control usage using the UPQC device.

Georgia et al. in [30] have shown that by using the phasor measurement unit data in the power system with the implementation of the FACTS devices the novel voltage control measurement is obtained. The authors proved the values of the simulated IEEE-68 test bus system and the IEEE-38 sample bus system after implementing the FACTS devices that the voltage being stable and controlled in different network topologies.

Yong et al. in [31] improved the control of the frequency in the high voltage transmission systems using deconcentrated control which is based on SVC devices. In order to have a preserving power system with realistic structure and voltage dependent loads a constraint that rely on strict Lyapunov energy function is utilized which used to design a nonlinear adaptive SVC controller. Which only need parameters and local bus measures. Also SVC along with a controller that is a conventional frequency droop. The control systems are tested on a standard 39-bus 10-machine power system and separated with conventional SVC controllers.

Sidnei et al. in [32] presented the optimal installed FACTS devices and the reactive power using a certain method. It can also enhance the voltage stability by changing decision variables of a power system with consideration to other indicators. This method was tested in standard studies using standard IEEE systems, and separate their result from the optimal methods that use probability and heuristic, one of them is the standard evolutionary algorithm. The results show the method has improved the stability of voltage for the systems and outdone the other methods.

Ghamgeen et al. in [33] presented the calculation of the practicability of compensating the power collapse on the power lines which reside in the Pakistani power transmission system by utilizing the FACTS devices and distributed generations. A 132 kV transmission system that gives the power to the Quetta electric supply company is being analyzed regarding the flow of the load and emergency. The results of simulation using NEPLAN in Baluchistan prove that the methods that are used have the ability to reduce the system losses, voltage variation and power flow congestion.

Bushra et al. in [34] proved that intelligent control schemes can defeat the limits of a fixed-parameter structure in Power System Stabilizers (PSS) for short and FACTS control along with additional control have a good chance in removing the variation.

Bazilah et al. in [35] presented the implementation of the current indices that are used in the existing techniques for correcting the best location and size issues in every kind of device that is called reactive power compensation. The existing literature survey for the best location and size is tested which contain approaches that are based on many things such as hybrid and systemic.

Chapter 3

METHODOLOGY

The methodology that have been used in this research will be discussed in this chapter. Formulas for voltage stability analysis technique that been used in the simulation is explained. Model for wind turbine as well as FACTS devices such as STATCOM and SVC explained, as well as the placement method of these FACTS devices are shown using a flow chart.

3.1 Voltage Stability Analysis Techniques

Voltage stability analysis techniques consist of two main analysis techniques, firstly static analysis and secondly dynamic analysis. Static analysis consists of firstly power flow study which is used to find the voltage magnitude and its phase angle also find the active/reactive power of each bus in the power system. Secondly, Q-V sensitivity is used to find the Eigenvalue for each bus and the participation factor for each bus with their Eigenvalue. Thirdly, P-V curve of each bus shows the relation of the voltage magnitude and the load parameter of the system. Lastly dynamic analysis showing the response time of the FACTS devices for if a disturbance happens in the system.

3.1.1 Power Flow

One of the power flow studies methods is the Newton Raphson method that is used to obtain the voltage magnitude and phase angle for each bus of the system as well as the active and reactive power of each bus. Using this method we can obtain the weakest bus of the system by finding the voltage profile of it. Using Newton Raphson method

is better than using other power flow methods such as Gauss Seidel method because of the quadratic convergence and its proven that its more efficient a big power system.

Newton Raphson method is done by firstly creating and calculating the Y-Bus matrix (admittance matrix) of the system and classify the slack bus voltage with its phase angle after that we do an estimation values for the voltages and phase angle for each bus and we set a counter for number of iteration and start with zero. Equation (3.1) and (3.2) are the equations which are used to find the new voltage and phase angle of the system where K is the number of iteration and i is the number of the bus. Where δ is the phase angle of voltage and θ is the phase angle from the Y-bus matrix.

$$P_k = \sum_{i=1}^n Y_{ki} V_i V_k \cos(\theta_{ki} + \delta_i - \delta_k) \quad (3.1)$$

$$Q_k = -\sum_{i=1}^n Y_{ki} V_i V_k \sin(\theta_{ki} + \delta_i - \delta_k) \quad (3.2)$$

The matrix equation (3.3) shown below where the first part is showing the incremental change of active and reactive power, in the middle is the jacobian matrix which is used to find the partial derivative for both of the Newton Raphson equations that are mentioned above respecting to voltage or phase angle, and the last part showing the incremental change of voltage magnitude and the phase angle. in equation (3.4) shows the incremental change of active and reactive power where the power that have been found from the iteraion after substituting the values of voltages and phase angle in equation (3.1) and (3.2) minus the values of the active and reactive power given from the system.

$$\begin{bmatrix} \Delta P_1^{(k)} \\ \vdots \\ \Delta P_n^{(k)} \\ \Delta Q_1^{(k)} \\ \vdots \\ \Delta Q_n^{(k)} \end{bmatrix} = \begin{bmatrix} \frac{\partial P_1^{(k)}}{\partial \delta_1} & \cdots & \frac{\partial P_1^{(k)}}{\partial \delta_n} & \frac{\partial P_1^{(k)}}{\partial V_1} & \cdots & \frac{\partial P_1^{(k)}}{\partial V_n} \\ \vdots & \ddots & \vdots & \vdots & \ddots & \vdots \\ \frac{\partial P_n^{(k)}}{\partial \delta_1} & \cdots & \frac{\partial P_n^{(k)}}{\partial \delta_n} & \frac{\partial P_n^{(k)}}{\partial V_1} & \cdots & \frac{\partial P_n^{(k)}}{\partial V_n} \\ \frac{\partial Q_1^{(k)}}{\partial \delta_1} & \cdots & \frac{\partial Q_1^{(k)}}{\partial \delta_n} & \frac{\partial Q_1^{(k)}}{\partial V_1} & \cdots & \frac{\partial Q_1^{(k)}}{\partial V_n} \\ \vdots & \ddots & \vdots & \vdots & \ddots & \vdots \\ \frac{\partial Q_n^{(k)}}{\partial \delta_1} & \cdots & \frac{\partial Q_n^{(k)}}{\partial \delta_n} & \frac{\partial Q_n^{(k)}}{\partial V_1} & \cdots & \frac{\partial Q_n^{(k)}}{\partial V_n} \end{bmatrix} \begin{bmatrix} \Delta \delta_1^{(k)} \\ \vdots \\ \Delta \delta_n^{(k)} \\ \Delta V_1^{(k)} \\ \vdots \\ \Delta V_n^{(k)} \end{bmatrix} \quad (3.3)$$

$$\begin{bmatrix} \Delta P_1^{(k)} \\ \vdots \\ \Delta P_n^{(k)} \\ \Delta Q_1^{(k)} \\ \vdots \\ \Delta Q_n^{(k)} \end{bmatrix} = \begin{bmatrix} P_1^{(k)} \\ \vdots \\ P_n^{(k)} \\ Q_1^{(k)} \\ \vdots \\ Q_n^{(k)} \end{bmatrix} - \begin{bmatrix} P_1 \\ \vdots \\ P_n \\ Q_1 \\ \vdots \\ Q_n \end{bmatrix} \quad (3.4)$$

Equation (3.4) showing the incremental change in active and reactive power by subtracting the active and reactive power that is obtained from iteration with the given values, where k means the counter for the number of iteration and n is the bus number. First part is the active and reactive power found after substituting the voltage and angle of the iteration, where the second part is the given active and reactive power of the system.

$$\begin{bmatrix} \Delta \delta_1^{(k)} \\ \vdots \\ \Delta \delta_n^{(k)} \\ \Delta V_1^{(k)} \\ \vdots \\ \Delta V_n^{(k)} \end{bmatrix} = - \begin{bmatrix} \frac{\partial P_1^{(k)}}{\partial \delta_1} & \cdots & \frac{\partial P_1^{(k)}}{\partial \delta_n} & \frac{\partial P_1^{(k)}}{\partial V_1} & \cdots & \frac{\partial P_1^{(k)}}{\partial V_n} \\ \vdots & \ddots & \vdots & \vdots & \ddots & \vdots \\ \frac{\partial P_n^{(k)}}{\partial \delta_1} & \cdots & \frac{\partial P_n^{(k)}}{\partial \delta_n} & \frac{\partial P_n^{(k)}}{\partial V_1} & \cdots & \frac{\partial P_n^{(k)}}{\partial V_n} \\ \frac{\partial Q_1^{(k)}}{\partial \delta_1} & \cdots & \frac{\partial Q_1^{(k)}}{\partial \delta_n} & \frac{\partial Q_1^{(k)}}{\partial V_1} & \cdots & \frac{\partial Q_1^{(k)}}{\partial V_n} \\ \vdots & \ddots & \vdots & \vdots & \ddots & \vdots \\ \frac{\partial Q_n^{(k)}}{\partial \delta_1} & \cdots & \frac{\partial Q_n^{(k)}}{\partial \delta_n} & \frac{\partial Q_n^{(k)}}{\partial V_1} & \cdots & \frac{\partial Q_n^{(k)}}{\partial V_n} \end{bmatrix}^{-1} \begin{bmatrix} \Delta P_1^{(k)} \\ \vdots \\ \Delta P_n^{(k)} \\ \Delta Q_1^{(k)} \\ \vdots \\ \Delta Q_n^{(k)} \end{bmatrix} \quad (3.5)$$

By using equation (3.5) the voltage and the phase angle will be obtained where the middle matrix is the inverse of the Jacobian matrix. The next iteration values will be

obtained by using equation (3.6) where k is the number of iterations. By using equation (3.6) the new iteration values will be found, and the power flow of the system is solved if the subtraction of the last two iterations are less than the tolerance value that is set in the system [36].

$$\begin{bmatrix} \delta_1^{(k+1)} \\ \vdots \\ \delta_n^{(k+1)} \\ V_1^{(k+1)} \\ \vdots \\ V_n^{(k+1)} \end{bmatrix} = \begin{bmatrix} \delta_1^{(k)} \\ \vdots \\ \delta_n^{(k)} \\ V_1^{(k)} \\ \vdots \\ V_n^{(k)} \end{bmatrix} + \begin{bmatrix} \Delta\delta_1^{(k)} \\ \vdots \\ \Delta\delta_n^{(k)} \\ \Delta V_1^{(k)} \\ \vdots \\ \Delta V_n^{(k)} \end{bmatrix} \quad (3.6)$$

3.1.2 Q-V Sensitivity

Q-V sensitivity is the voltage stability analysis of the system by using the eigenvalues of the Jacobian matrix. By using the eigenvalues of the Jacobian matrix we can classify the location of buses that is close to the collapse point and the location where the reactive power need to be injected to it. The stability of voltage in the power system is affected mainly from the reactive power variation which mean that the active power is mostly constant at every operating point, when considering P to be constant we can find that $\Delta P = 0$. using this in equation (3.1) we end up with:

$$\Delta Q = J_R \Delta V \quad (3.7)$$

Where J_R is the reduced Jacobian matrix which is obtained as the following:

$$J_R = \begin{bmatrix} J_{QV} - J_{Q\theta} J_{P\theta}^{-1} J_{PV} \end{bmatrix} \quad (3.8)$$

Where J_{QV} is the partial derivative of the reactive power respect to the voltage magnitude, $J_{Q\theta}$ is the partial derivative of the reactive power respect to the voltage phase angle, $J_{P\theta}^{-1}$ is the inverse partial derivative of the active power respect to the

voltage phase angle and J_{pV} is the partial derivative of the active power respect to the voltage magnitude. The eigenvector and the eigenvalue of the reduced Jacobian matrix in the power network can be defined as:

$$J_R = \xi \Lambda \eta \quad (3.9)$$

Where is ξ the right eigenvector of the reduced Jacobian matrix, Λ is the diagonal eigenvalue matrix of the reduced Jacobian matrix and η is the left eigenvector of the reduced Jacobian matrix. Equation (3.10) shows the inverse of the reduced Jacobian matrix.

$$J_R^{-1} = \xi \Lambda^{-1} \eta \quad (3.10)$$

Substitute equation (3.10) in equation (3.7) we end up with:

$$\Delta V = (\xi \Lambda^{-1} \eta) \Delta Q \quad (3.11)$$

$$\Delta V = \sum_i \frac{\xi_i \eta_i}{\lambda_i} \Delta Q \quad (3.12)$$

Where is ξ_i the i th right eigenvector of the reduced Jacobian matrix, η_i is the i th left eigenvector of the reduced Jacobian matrix and λ_i is the i th eigenvalue which found from the diagonal matrix Λ^{-1} . Equation (3.13) shows the i th modal voltage.

$$\Delta V_{mi} = \frac{1}{\lambda_i} \Delta Q_{mi} \quad (3.13)$$

Where is ΔQ_{mi} expressed in equation (3.14) is the i th modal reactive power variation, and K_i is the normalization factor.

$$\Delta Q_{mi} = K_i \xi_i \quad (3.14)$$

Voltage stability analysis is done by using the eigenvalue of the reduced Jacobian matrix, the system will be considered unstable if a negative or equal to zero eigenvalue

have been found in the analysis, meaning that by equation (3.15) the smaller positive λ_i the closer the system to be unstable. If any eigenvalue has a positive real part, the system will tend to move to steady state point (stable system), as well as If any eigenvalue has a negative real part, the system will tend to move back away from steady state point (stable system). If any eigenvalue has an imaginary part, the system oscillate around the steady state point.

$$\frac{\Delta V_k}{\Delta Q_k} = \sum_i \frac{\xi_{ki} \eta_{ik}}{\lambda_i} \quad (3.15)$$

$$P_{ki} = \xi_{ki} \eta_{ik} \quad (3.16)$$

Participation factor of most associated buses of k th bus in the i th mode is found by using equation (3.16) where it refers to the bus participation factor, because of the power flow nonlinearity the eigenvalue magnitude cannot give the best measure to voltage stability [37].

3.1.3 P-V Curve

Continuation power flow is used to find the P-V curve for the system, continuation algorithm is mathematical approach used to solve the nonlinear equations. The solution branch can be controlled around the turning point using the continuation algorithm without difficulty which make the continuation algorithm more useful for the power system in approximations of the critical point.

$$\Delta P_i = P_{Gi}(\lambda) - P_{Li}(\lambda) - P_{Ti} = 0 \quad (3.17)$$

$$\Delta Q_i = Q_{Gi}(\lambda) - Q_{Li}(\lambda) - Q_{Ti} = 0 \quad (3.18)$$

In (3.17) and (3.18) is the continuation power flow equations where is P_{Ti} and Q_{Ti} is shown in equations (3.1) and (3.2) respectively, where is ΔP_i , $P_{Gi}(\lambda)$ and $P_{Li}(\lambda)$ respectively is the incremental change in the active power at bus (i), active generation

power at bus (i) and active load power at bus (i). ΔQ_i , $Q_{Gi}(\lambda)$ and $Q_{Li}(\lambda)$ respectively is the incremental change in the reactive power at bus (i), reactive generation power at bus (i) and reactive load power at bus (i). Where λ corresponds to the loading parameter [38].

Figure (3.1) shows the P-V curve analysis where it shows the relation between the voltage magnitude variation and the active power. The critical point is the maximum value for the loading parameter before the system collapse which called the bifurcation point. voltage stability margin is located between the operating point and the bifurcation point which correspond to the stability margin.

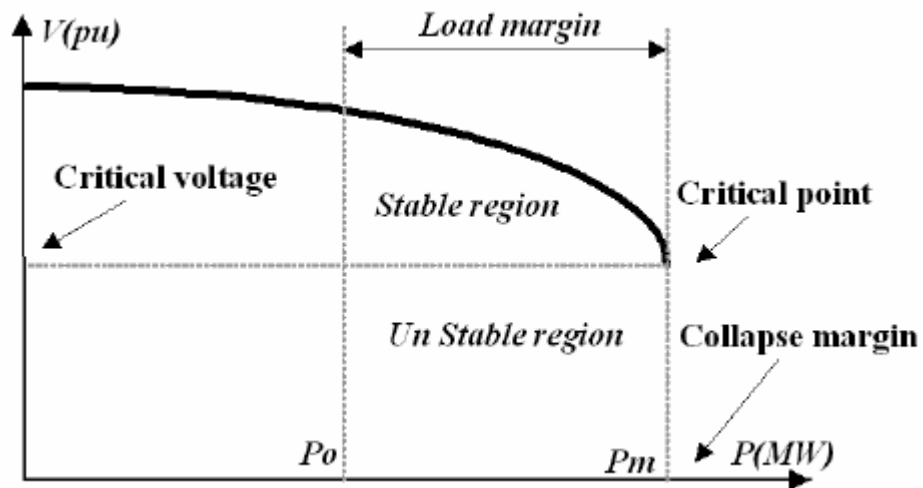


Figure 3.1: P-V curve analysis

3.1.4 Dynamic Analysis

Time domain simulation is performed on the power system and its components. Where the component of the power system can be shown as a set of nonlinear algebraic equations, using the time integration method such as trapezoidal rule for solving these nonlinear algebraic equations.

Trapezoidal rule is a numerical analysis method where it solve the linear and nonlinear differential equations. If we suppose we have the function $Y' = f(T, Y)$ and it's a nonlinear algebraic equation the trapezoidal equation is given by (3.19) where h is the step size $h = T_{n+1} - T_n$ [39].

$$Y_{n+1} = Y_n + \frac{1}{2}h(f(T_n, Y_n) + f(T_{n+1}, Y_{n+1})) \quad (3.19)$$

3.2 FACTS Devices

Static controller and power system electronic devices called flexible alternating current transmission system devices used for enhance the capability of power transfer in the system and improve the controllability of the power system. They can absorb and supply the reactive and active powers by interfering with the energy storage element and they can control the dynamic condition of the system due to the fast operation of these devices. In this thesis, STATCOM and SVC are implemented to enhance the power system voltage profile and prevent the system form collapse.

3.2.1 STATCOM Device

Static Synchronous Compensator (STATCOM) is a fast reacting device connected with the load in parallel, and its job is to provide or absorb the active and reactive power in the system as well as maintaining the voltage profile of the system in an acceptable limit. The definition of STATCOM can be fragmented into three components. Firstly, it is static which implies it has no rotational part and is based on solid state switches. Secondly, it is synchronous which is related to three phase synchronous machines. Thirdly, compensator can be seen as providing reactive power support.

In figure (3.2) show the module of STATCOM where the STATCOM connected with

the weakest bus with an ideal shunt-connected transformer and also show the VSC which refers to the voltage source converter which is one of the most important parts in STATCOM, the active power between the VSC and the AC source is controlled using the phase angle, and the reactive power is found by using the voltage magnitude of the source (V_K) and the output fundamental voltage of VSC (V_{VR}). If $V_{VR} > V_K$ the reactive power will be generated by VSC and if $V_{VR} < V_K$ the reactive power will be consumed by VSC. STATCOM have many of advantages such as: the fast response time as well as the small size and the changeable characteristics for different operation conditions [40].

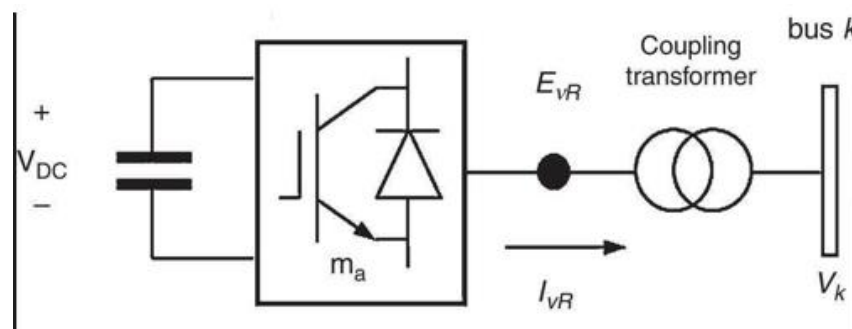


Figure 3.2: STATCOM model

3.2.2 SVC Device

Static Var Compensator (SVC) work as a generator where it can absorb or generate reactive power to the power system when it's connected with the load in parallel. Thyristor controlled reactor is a part of SVC where it is connected in parallel with the bank of capacitors as shown in figure (3.3). SVC control the voltage magnitude of the power system at the connection point by absorbing or generating reactive power to the point of connection to network, as well as it support the voltage regulation and the reactive power in the system. The instantaneous speed of the SVC response is provided from the angle control fired from thyristor. Which is an important component for the

voltage magnitude control [40].

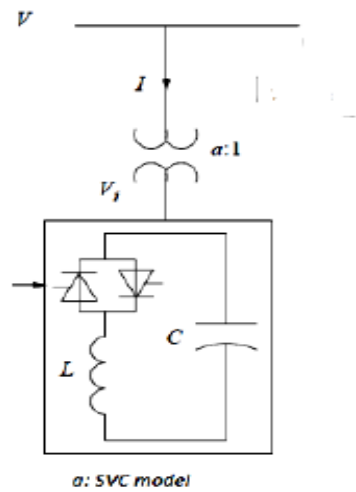


Figure 3.3: SVC model

3.3 FACTS Devices Placement Method

Static analysis of the system is used as the algorithm for the FACTS devices placement in the power system, a flow chart in figure (3.4) shows the procedure of placement STATCOM and SVC in the power system using the data from the voltage stability analysis. Voltage stability analysis is used to determine the weakest bus in the system and the FACTS devices are implemented on the weakest bus for the enhancement of the voltage profile and power system stability.

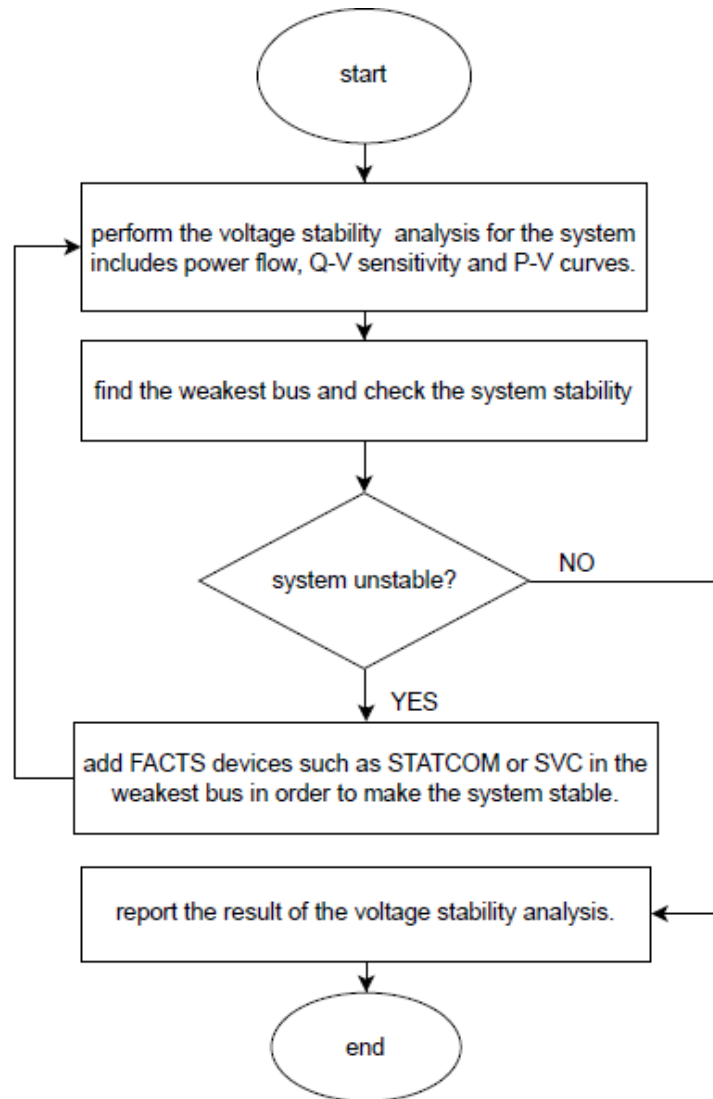


Figure 3.4: Flow chart for placement method

3.4 Wind Farm Modeling

Wind turbine is a device which generates electricity by feeding the generator kinetic energy generated from the wind turbine movement from air. Wind turbine have two axis vertical and horizontal axis, vertical axis is when the blades rotate perpendicular to the ground, on the other hand, horizontal axis is when the blades rotate parallel to the ground. Doubly-Fed Induction Generator (DFIG) is one of the main parts of the wind farm model because of the many advantages the (DFIG) have such as, the ability of electricity production in a low wind speed, the high efficacy comparing with other

generators and the ability of control the amount of absorbed or supplied reactive power to the grid by controlling the power factor.

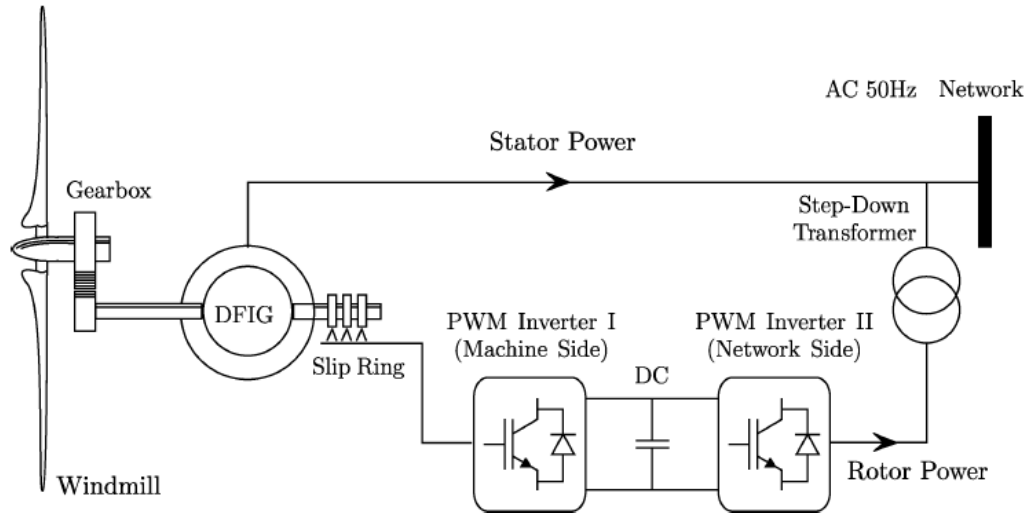


Figure 3.5: DFIG equipped wind turbine diagram

Figure (3.5) shows a diagram of Doubly-Fed Induction Generator (DFIG) equipped wind turbine. Stator power is connected from DFIG to the grid, where the stator winding is connected to the DFIG through back to back voltage source converter which contain pulse width modulated (PWM) inverter and via slip ring. Pulse width modulated (PMW) is an inverter which depend on the pulse width modulation technology and its used to give a steady output voltage as the desired voltages relaying on the load connected and the country irrespective, it used also to convert the high DC voltage to standard AC. Slip ring is a device where allow the electrical signal and the power transmission from the stationary to a rotating structure. The magnetic field, produced in the rotor windings, rotates due to the rotation of the generator's rotor plus the rotational effects produced by the converter AC current. This gives rise to two possibilities where the rotor's magnetic field rotates opposite and in the same direction as the rotor. Super-synchronous operation occurs when the rotor magnetic field is in the same direction as the generator rotor. Sub-synchronous operation occurs when the

rotor magnetic field is in the opposite direction of the generator rotor [41].

3.5 PSAT Software

PSAT refers to power system analysis toolbox, which is an open source toolbox in Matlab that can be used for power system analysis and control learning, education and research. PSAT have many features such as Power Flow; Continuation Power Flow; Optimal Power Flow; Small Signal Stability Analysis; Time Domain Simulation; FACTS Models; Wind Turbine Models.

Figure 3.6 shows the main page of power system analysis toolbox where the test power system can be load in PSAT using the data file option. After the power system is loaded, voltage stability analysis can be calculated for the power system using the option power flow in order to find the voltage magnitude and its phase angle as well as active and reactive power of the system. CPF refers to Continuation power flow is used to calculate the P-V curve for each bus of the power system, while eigenvalues are calculated from the eigenvalues analysis option shown in the figure.

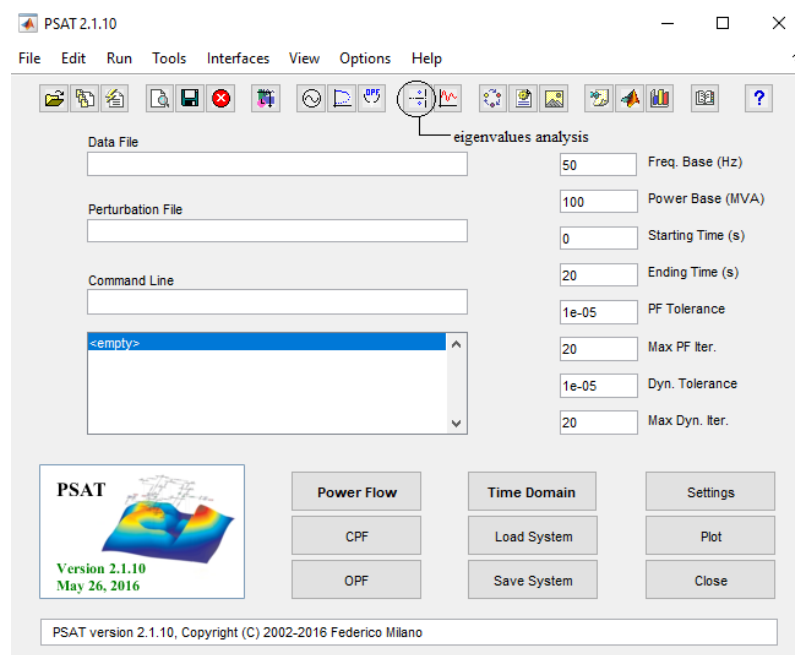


Figure 3.6: Main page of PSAT

Figure 3.7 shows the PSAT plot page where it shows the voltage magnitude for each bus in the power system to be on the y-axis as well as show the options in terms of time and many other values to be on x-axis. By using the plot option a graph will be plotted such as P-V curves of the buses is plotted after the Continuation power flow is calculated, as well as the voltage magnitude fluctuation during time after the time domain simulation.

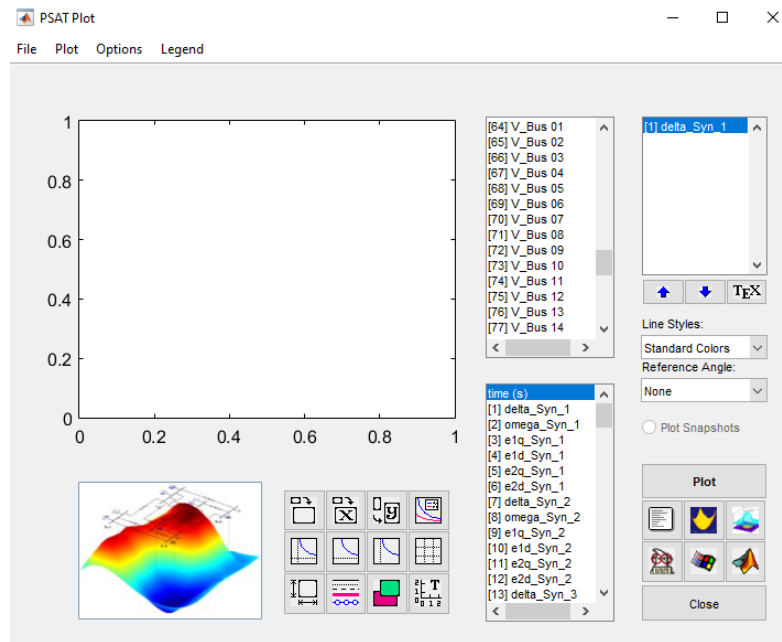


Figure 3.7: PSAT plot page

Chapter 4

RESULT AND DISCUSSION

4.1 Case Study (IEEE 14- Bus Test System)

A 14- bus system is used to show the effect of adding FACTS devices on the voltage profile and system stability. The approached methodology is explained by using the 14-bus case in figure 4.1. power system contain four generator and a wind farm lies on the bus one which is the slack bus too and have 11 load on different buses . The target voltage of the system is shown depending on the ANSI standard C84.1 guidelines [41]. which is shown in table 4.1, tow ranges, rage A show the optimal and the best voltage limit for voltage above 46 KV, where is range B shows the acceptable limit of voltage under 46 KV. Table 4.1 show the voltage magnitude limits for both ranges where range 1 is the normal operating condition while range 2 is the emergency condition.

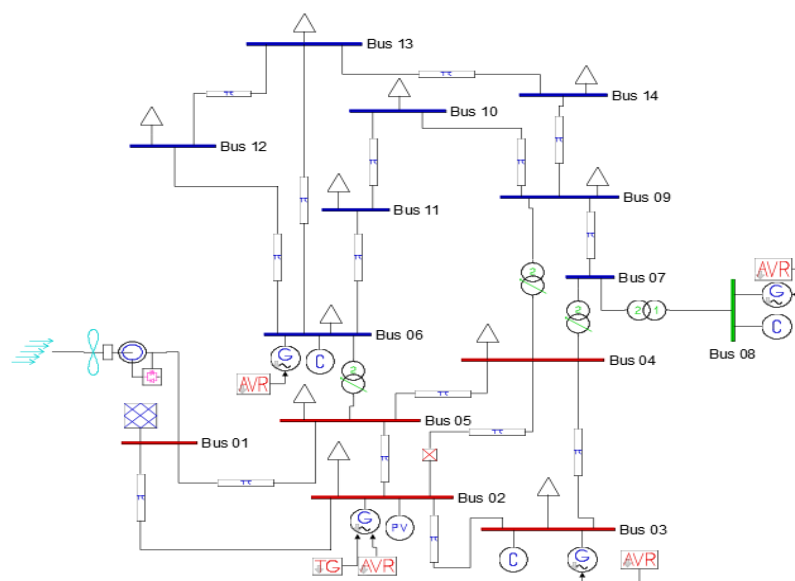


Figure 4.1: IEEE 14-bus test system

Table 4.1: Two ranges of Voltage levels, depending on ANSI C84.1

Voltage levels	Range 1		Range 2	
	Minimum rate (p.u.)	Maximum rate (p.u.)	Minimum rate (p.u.)	Maximum rate (p.u.)
2.4 KV – 35.4 KV	0.9750	1.050	0.950	1.0580
Above 46 KV	Normal condition		Emergency condition	
	Minimum rate (p.u.)	Maximum rate (p.u.)	Minimum rate (p.u.)	Maximum rate (p.u.)
	0.95	1.06	0.90	1.10

4.2 Voltage Stability Analysis

4.2.1 Voltage Stability Analysis for Power System without FACTS (Case 1)

Firstly, a detail power flow study result of the power system is shown in table 4.2 before adding the STATCOM or SVC devices on the system. By using the Newton Raphson algorithm the table shows the voltage magnitude of each bus and its phase angle along with active and reactive power. We can see that in bus 1 reactive power generation is in minus which shows the effect of DFIG in absorbing reactive power and also showed the weakest buses of the system, which have the lowest voltage magnitude such as bus 14, bus 9 and bus 4. Where the voltage magnitude in these buses are not on acceptable or desired limit which can cause a black out of the power system.

Table 4.2: Power flow result without compensator

Bus number	Bus type	Voltage (pu)	Angle (rad)	P generation (pu)	Q generation (pu)	P load (pu)	Q load (pu)
01	SLACK	1.06	0.00	8.4533	-0.01705	0.00	0.00
02	PV	1.045	-0.34054	0.4	3.8366	0.6076	0.3556
03	PV	1.01	-0.78389	0.00	2.1434	2.6376	0.532
04	PQ	0.91961	-0.62317	0.00	0.00	1.3384	0.112
05	PQ	0.92471	-0.53621	0.00	0.00	0.2128	0.0448
06	PV	1.07	-0.87017	0.00	1.5766	0.3136	0.21
07	-	0.96784	-0.79527	0.00	0.00	0.00	0.00
08	PV	1.09	-0.79527	0.00	0.75593	0.00	0.00
09	PQ	0.91726	-0.88776	0.00	0.00	0.826	0.4648
10	PQ	0.9205	-0.90088	0.00	0.00	0.252	0.1624
11	PQ	0.98337	-0.89075	0.00	0.00	0.098	0.0504
12	PQ	1.0169	-0.91451	0.00	0.00	0.1708	0.0448
13	PQ	0.99347	-0.91615	0.00	0.00	0.378	0.1624
14	PQ	0.89046	-0.96333	0.00	0.00	0.4172	0.14

Table 4.3 shows the results of Q-V modal analysis that performed on system. It shown that all eigenvalues are positive and have no imaginary part indicate that the power system is stable, meaning that the smaller the positive eigenvalue is the more instability the power system and it also show the bus participation factor that is associated with the eigenvalues, it shown that eigenvalue number 9 is the smallest which is (0.26833) that is associated with the bus 14 with participation factor (0.13202), showing that bus 14 is the weakest bus of them and the one which leading to voltage instability.

Table 4.3: Q-V model analysis without compensator

Eigenvalue number	Most Associated Bus	Eigenvalue (real part)	Eigenvalue (imaginary part)	Participation factor
1	04	59.3674	0.00	0.53321
2	02	49.377	0.00	0.70221
3	09	35.08	0.00	0.57236
4	06	29.6977	0.00	0.69844
5	07	21.9651	0.00	0.31308
6	07	18.2953	0.00	0.16087
7	13	15.9602	0.00	0.36872
8	03	14.3652	0.00	0.63335
9	14	0.26833	0.00	0.13202
10	11	11.3653	0.00	0.34021
11	12	2.9419	0.00	0.21655
12	12	3.7196	0.00	0.15549
13	08	6.2761	0.00	0.53623
14	14	5.5814	0.00	0.62397

The third analysis done for the power system is the V-P curve analysis. The results indicate the relation between the voltage magnitude and the loading parameter (λ) in per unit for each bus in the system, loading parameter shows the Load ability limits are critical points of particular interest in voltage stability assessment, indicating how much a system can be stressed from a given state before reaching instability., in the figures shown below its found to be 1.5. Figure 4.2 showing the first five buses of the system knowing that the bus1, bus2 and bus 3 are PV buses have constant voltage, also shows the loading margin for bus4 and bus5, voltage magnitude drop to 0.71 at the nose point before the collapse happens.

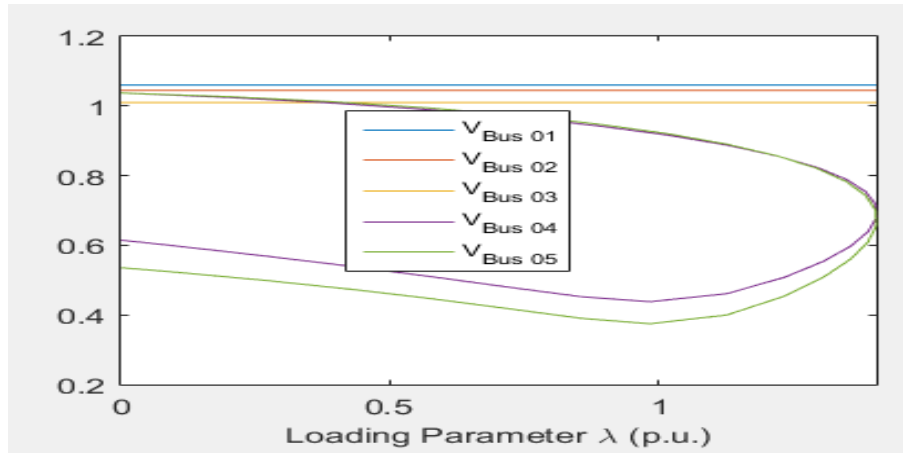


Figure 4.2: P-V curve for voltage at bus 1-bus 5

Figure 4.3 shows the PV curve analysis for buses 6-10 showing the voltage magnitude drop I during the increasing in loading parameters reaching about 1.5 and collapse, we can see bus9 as the weakest since it have the lowest nose point and keep going down to 0.47 and bus10 have a better nose point but collapse to about 0.44. The curve of the last four buses is shown in figure 4.4 showing that also bus14 is the weakest among them having the lowest nose point and keep dropping the voltage magnitude reaching 0.48 after collapse.

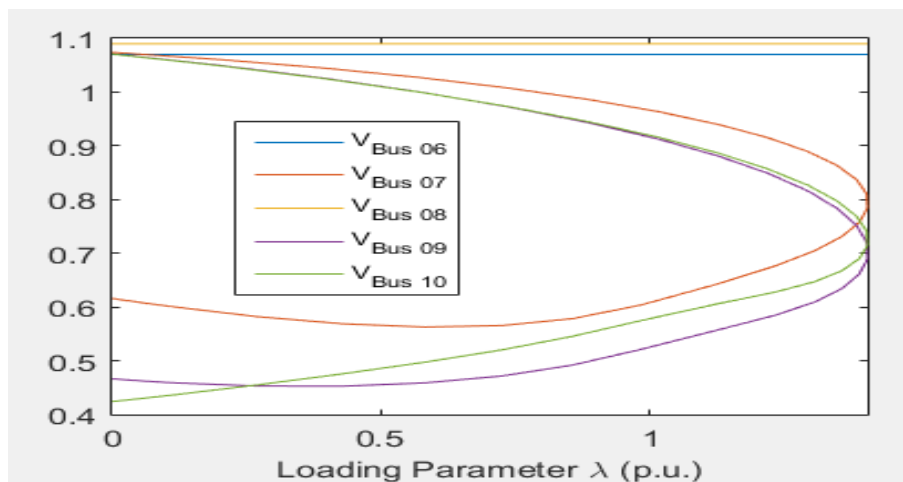


Figure 4.3: P-V curve for voltage at bus 6-bus 10

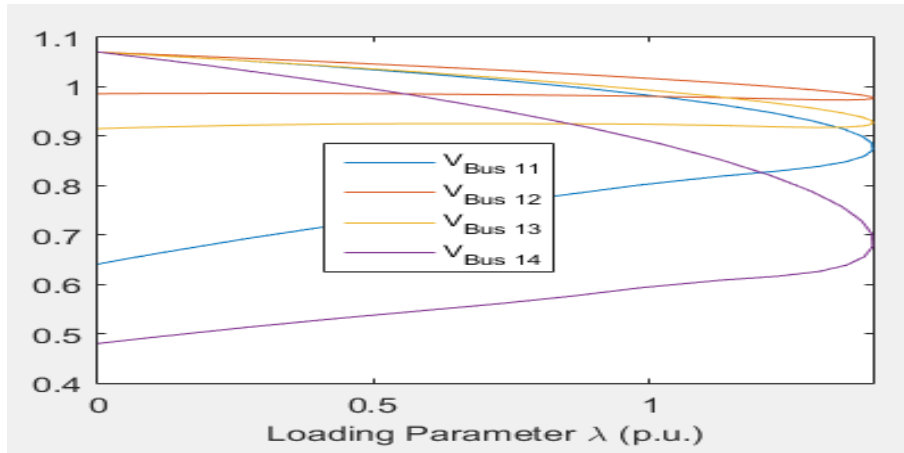


Figure 4.4: P-V curve for voltage at bus 11-bus 14

4.2.2 Voltage Stability Analysis for Power System with STATCOM at Bus 14 (Case 2)

One of the FACTS devices which is static synchronous compensator (STATCOM) is implemented on bus 14 as the first case to do the voltage stability analysis for. Table 4.4 shows the power flow result of the system after the implementation, we can notice the huge enhancement on the voltage profile for all the buses on the system. Bus 14 was the weakest having 0.89046 p. voltage magnitude before the compensation and after the compensation it have 1.03 p.u. voltage magnitude which specify that voltage profile is stable and improved for power system. As well as it can be noticed the active and reactive power generation in bus 14 after implementing the STATCOM on it.

Table 4.4: Power flow result with STATCOM on bus 14

Bus number	Voltage (pu)	Angle (rad)	P generation (pu)	Q generation (pu)	P load (pu)	Q load (pu)
01	1.06	0.00	6.2992	-0.36713	0.00	0.00
02	1.045	-0.25472	0.4	2.4549	0.6076	0.3556
03	1.01	-0.63617	0.00	1.8086	2.6376	0.532
04	0.96591	-0.44747	0.00	0.00	1.3384	0.112
05	0.97537	-0.37758	0.00	0.00	0.2128	0.0448
06	1.07	-0.52761	0.00	1.2307	0.3136	0.21
07	0.9938	-0.49365	0.00	0.00	0.00	0.00
08	1.09	-0.49365	0.00	0.59528	0.00	0.00
09	0.93782	-0.51923	0.00	0.00	0.826	0.4648
10	0.93815	-0.53699	0.00	0.00	0.252	0.1624
11	0.99284	-0.53814	0.00	0.00	0.098	0.0504
12	1.0226	-0.53774	0.00	0.00	0.1708	0.0448
13	1.0184	-0.50635	0.00	0.00	0.378	0.1624
14	1.03	-0.30753	1.6	0.11368	0.4172	0.14

Table 4.5 shows the Eigenvalues of the system with participation factor of the most associated buses, its noticed the increase in the weakest and lowest eigenvalue buses meaning that the system stability increased. Figures (4.5), (4.6) and (4.7) show the P-V curve after the implementation in bus 14, where the load parameter is increased reaching about 1.85p.u. meaning that the system can handle more load increment before reaching to the collapse point which is the nose point of the curves as well as show that the buses maintain a high voltage magnitude after the collapse point where the load start decreasing in the system.

Table 4.5: Q-V model analysis result with STATCOM on bus 14

Eigenvalue number	Most Associated Bus	Eigenvalue (real part)	Eigenvalue (imaginary part)	Participation factor
1	04	62.7118	0.00	0.52913
2	02	50.2823	0.00	0.70381
3	09	35.8841	0.00	0.57352
4	06	30.0299	0.00	0.68702
5	07	22.8267	0.00	0.27593
6	07	18.8817	0.00	0.20643
7	13	16.2521	0.00	0.39118
8	03	14.7108	0.00	0.67795
9	14	1.1505	0.00	0.23737
10	11	11.4879	0.00	0.34192
11	12	3.0429	0.00	0.17186
12	14	3.7501	0.00	0.19024
13	08	6.3269	0.00	0.53157
14	14	5.0516	0.00	0.399

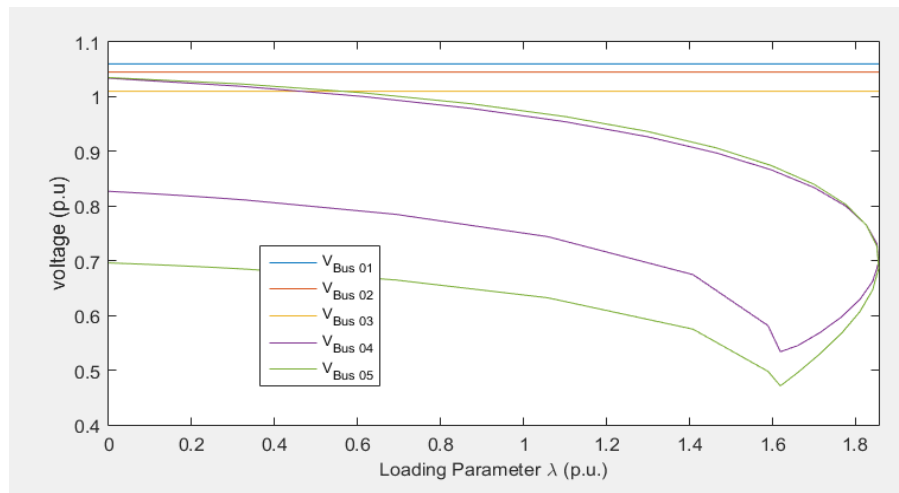


Figure 4.5: P-V curve after compensation for voltage at bus 1-bus 5

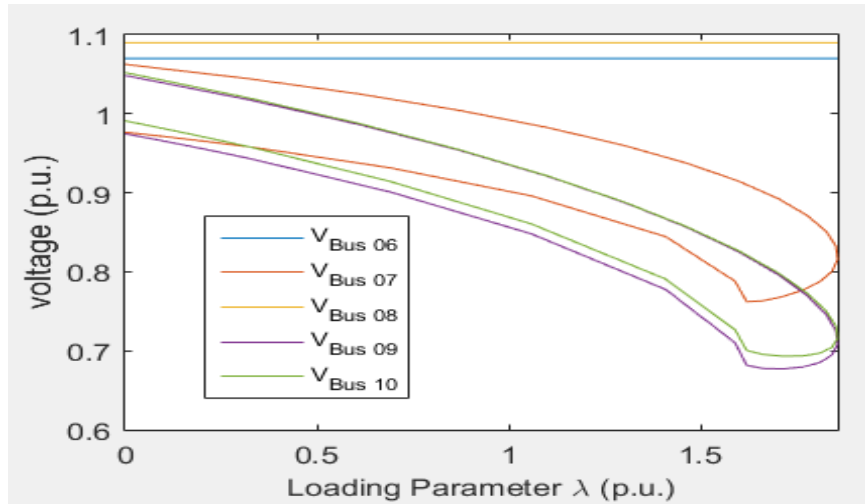


Figure 4.6: P-V curve after compensation for voltage at bus 6-bus 10

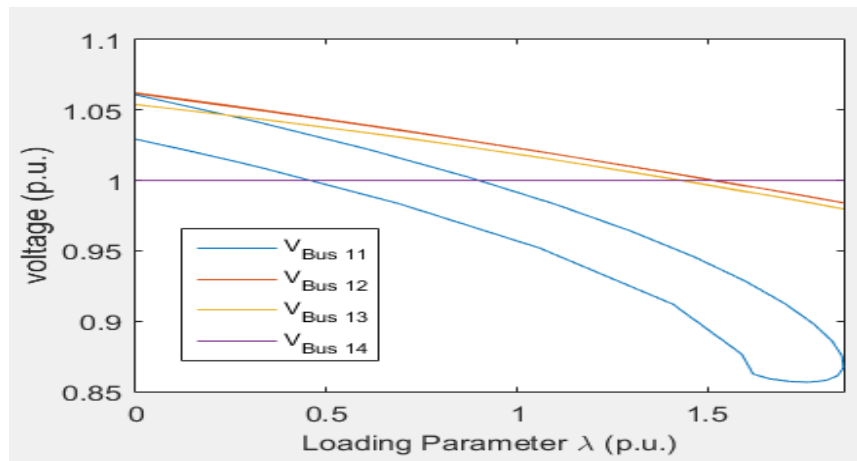


Figure 4.7: P-V curve after compensation for voltage at bus 11-bus 14

4.2.3 Voltage Stability Analysis for Power System with STATCOM at Bus 9 (Case 3)

Static synchronous compensator (STATCOM) in this case is implemented on bus 9 which is the second weakest bus in the power system, voltage stability analysis for this case is shown below, where Table 4.6 shows the power flow result of the system after the implantation in bus 9, we can notice active and reactive power generation in bus 9 where it enhance the voltage magnitude for bus 9 to be 1.03 p.u. and the voltage magnitude in all buses making the system more reliable and improve the voltage profile. Table 4.7 shows the Eigenvalues of the system with participation factor of the

most associated buses, it's noticed the enhancement of the Q-V sensitivity values such as increase in the eigenvalues. Figures (4.8), (4.9) and (4.10) show the P-V curve after the implementation in bus 9, where the load parameter is increased reaching 2p.u. meaning that the system can handle more load increment before reaching to the collapse point which is the nose point of the curves as well as show that the buses maintain a high voltage magnitude after the collapse point when the high load release.

Table 4.6: Power flow result with STATCOM on bus 9

Bus number	Voltage (pu)	Angle (rad)	P generation (pu)	Q generation (pu)	P load (pu)	Q load (pu)
01	1.06	0.00	6.1776	-0.39093	0.00	0.00
02	1.045	-0.24878	0.4	2.2889	0.6076	0.3556
03	1.01	-0.62216	0.00	1.7217	2.6376	0.532
04	0.97892	-0.43429	0.00	0.00	1.3384	0.112
05	0.98146	-0.37308	0.00	0.00	0.2128	0.0448
06	1.07	-0.56533	0.00	1.0792	0.3136	0.21
07	1.0264	-0.44329	0.00	0.00	0.00	0.00
08	1.09	-0.44329	0.00	0.39386	0.00	0.00
09	1.03	-0.44803	1.6	0.1966	0.826	0.4648
10	0.99058	-0.48452	0.00	0.00	0.252	0.1624
11	1.0202	-0.5316	0.00	0.00	0.098	0.0504
12	1.0224	-0.59957	0.00	0.00	0.1708	0.0448
13	1.008	-0.59289	0.00	0.00	0.378	0.1624
14	0.94517	-0.56763	0.00	0.00	0.4172	0.14

Table 4.7: Q-V model analysis result with STATCOM on bus 9

Eigenvalue number	Most Associated Bus	Eigenvalue (real part)	Eigenvalue (imaginary part)	Participation factor
1	04	63.3603	0.00	0.53308
2	02	50.3512	0.00	0.70395
3	09	37.1715	0.00	0.56485
4	06	30.0531	0.00	0.68662
5	07	23.2966	0.00	0.3153
6	14	0.97606	0.00	0.13658
7	07	19.23	0.00	0.1767
8	13	16.283	0.00	0.39718
9	03	14.7375	0.00	0.68126
10	11	11.6376	0.00	0.32843
11	12	3.5063	0.00	0.29125
12	01	3.9533	0.00	0.15295
13	08	6.403	0.00	0.55558
14	14	5.9443	0.00	0.62163

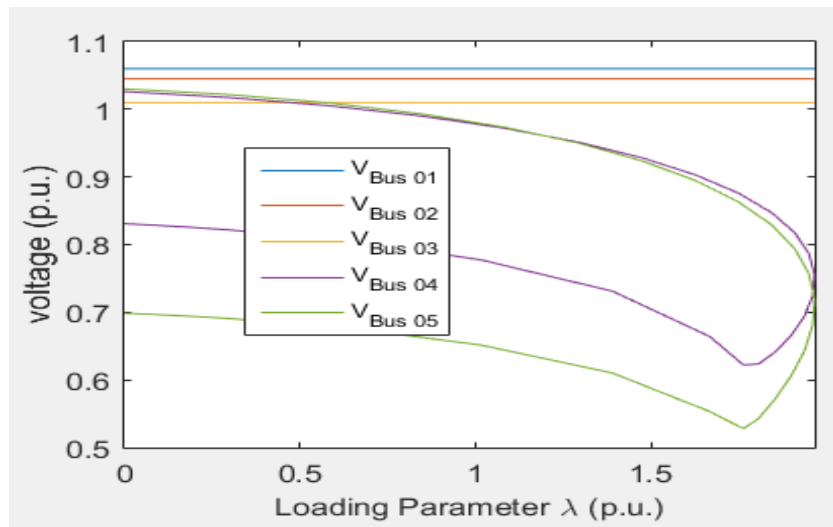


Figure 4.8: P-V curve after compensation for voltage at bus 1-bus 5

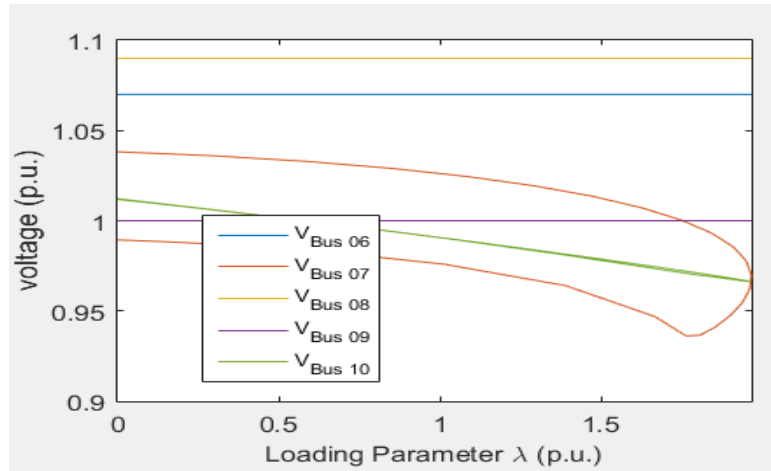


Figure 4.9: P-V curve after compensation for voltage at bus 6-bus 10

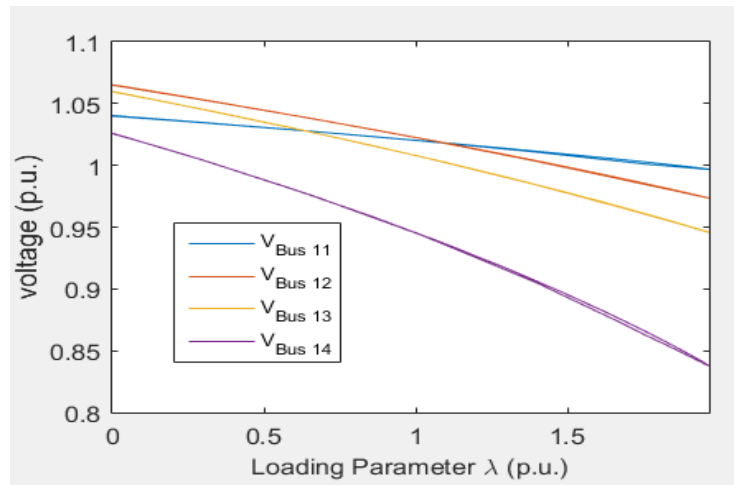


Figure 4.10: P-V curve after compensation for voltage at bus 11-bus 14

4.2.4 Voltage Stability Analysis for Power System with STATCOM at Bus 4 (Case 4)

Static synchronous compensator (STATCOM) in this case is implemented on bus 4 which is the third weakest bus in the power system, voltage stability analysis for this case is shown below, where Table 4.8 shows the power flow result of the system after the implantation in bus 4, we can notice active and reactive power generation in bus 4 where it enhance the voltage magnitude for bus 4 to be 1.03 p.u. and the voltage profile enhanced in the power system. But because of the far distance between the bus 4 and the bus 14 as well as the power loss in the transmission system the voltage magnitude

in the bus 14 still low and not acceptable as shown below in the power flow table. Table 4.9 shows the Eigenvalues of the system with participation factor of the most associated buses, the results show that the system is stable but the values are low meaning the system is stable but not secure from collapse if an increase in the load happen. Figures (4.11). (4.12) and (4.13) show the P-V curve after the implementation in bus 4, where the load parameter is increased reaching 2 p.u. meaning that the system can handle more load increment before reaching to the collapse point which is the nose point of the curves but its also noticed that the bus 14 after reaching the nose point the bus voltage magnitude keep going down reaching to zero.

Table 4.8: Power flow result with STATCOM on bus 4

Bus number	Voltage (pu)	Angle (rad)	P generation (pu)	Q generation (pu)	P load (pu)	Q load (pu)
01	1.06	0.00	6.1435	-0.41398	0.00	0.00
02	1.045	-0.24525	0.4	2.0878	0.6076	0.3556
03	1.01	-0.60893	0.00	1.5824	2.6376	0.532
04	1.03	-0.4254	1.6	0.8425	1.3384	0.112
05	0.98819	-0.3785	0.00	0.00	0.2128	0.0448
06	1.07	-0.66874	0.00	1.1241	0.3136	0.21
07	1.0066	-0.5864	0.00	0.00	0.00	0.00
08	1.09	-0.5864	0.00	0.51621	0.00	0.00
09	0.95695	-0.67663	0.00	0.00	0.826	0.4648
10	0.95417	-0.69094	0.00	0.00	0.252	0.1624
11	1.001	-0.68558	0.00	0.00	0.098	0.0504
12	1.0201	-0.71164	0.00	0.00	0.1708	0.0448
13	1.0002	-0.71308	0.00	0.00	0.378	0.1624
14	0.91764	-0.75224	0.00	0.00	0.4172	0.14

Table 4.9: Q-V model analysis result with STATCOM on bus 4

Eigenvalue number	Most Associated Bus	Eigenvalue (real part)	Eigenvalue (imaginary part)	Participation factor
1	05	60.6301	0.00	0.50402
2	02	50.3919	0.00	0.70561
3	09	36.5306	0.00	0.57879
4	06	29.6944	0.00	0.70207
5	07	22.362	0.00	0.3895
6	04	0.45922	0.00	0.11499
7	13	18.124	0.00	0.16399
8	13	16.0234	0.00	0.3372
9	03	14.6843	0.00	0.59262
10	11	11.6011	0.00	0.32699
11	12	2.9067	0.00	0.18289
12	12	3.6901	0.00	0.19007
13	08	6.3483	0.00	0.54456
14	14	5.7657	0.00	0.6359

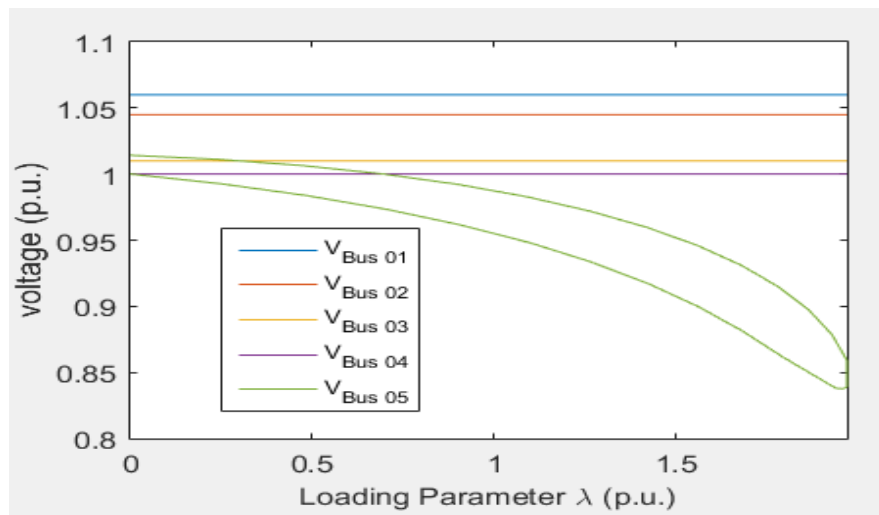


Figure 4.11: P-V curve after compensation for voltage at bus 1-bus 5

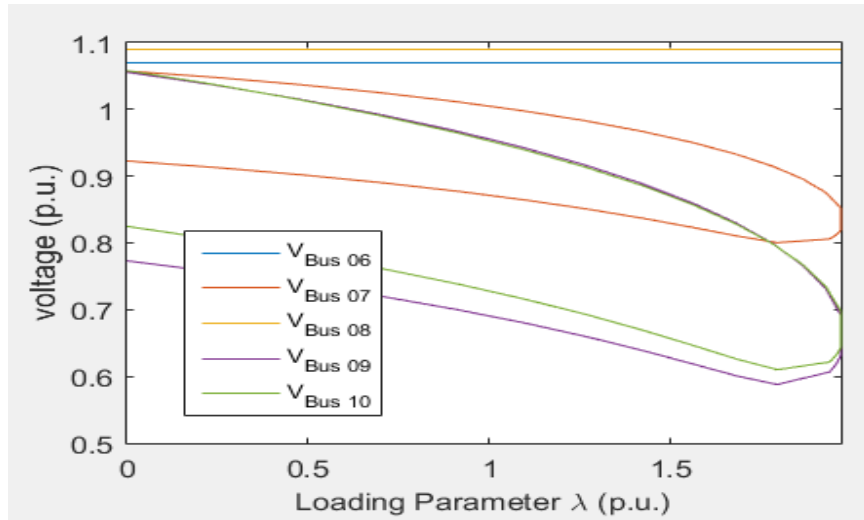


Figure 4.12: P-V curve after compensation for voltage at bus 6-bus 10

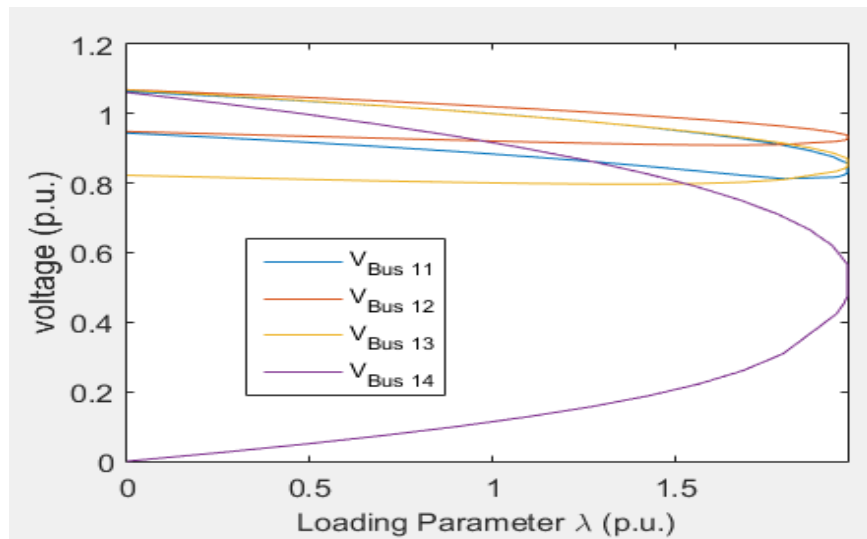


Figure 4.13: P-V curve after compensation for voltage at bus 11-bus 14

4.2.5 Voltage Stability Analysis for Power System with SVC at Bus 14 (Case 5)

A Static Var Compensator (SVC) device is implemented in case 5, case 6 and case 7 where SVC in the first case implemented on bus 14 to do the voltage stability analysis for the power system after compensation. Table 4.10 shows the power flow result of the system after the implantation of SVC device, we can notice the huge enhancement on the voltage profile for all the buses on the system as well as the active and reactive power generation from bus 14 have been noticed. Bus 14 voltage magnitude after the

consumption is 1.03 p.u. Meaning that the voltage profile is improved and the power system is more stable. Table 4.11 shows the Eigenvalues of the system with participation factor for each bus, Q-V sensitivity values show that the eigenvalues of the power system have been increased after the compensation meaning that the power system is more stable. Figures (4.14), (4.15) and (4.16) show the P-V curve after the implementation of SVC device in bus 14, where the load parameter is increased reaching 1.8 p.u. meaning that the system can handle more load increment before reaching to the collapse point which is the nose point of the curves as well as returning the voltage magnitude to normal values after the nose point.

Table 4.10: Power flow result with SVC on bus 14

Bus number	Voltage (pu)	Angle (rad)	P generation (pu)	Q generation (pu)	P load (pu)	Q load (pu)
01	1.06	0.00	6.7404	-0.32662	0.00	0.00
02	1.045	-0.27184	0.4	2.6804	0.6076	0.3556
03	1.01	-0.66501	0.00	1.8528	2.6376	0.532
04	0.95977	-0.48334	0.00	0.00	1.3384	0.112
05	0.96785	-0.40971	0.00	0.00	0.2128	0.0448
06	1.07	-0.59438	0.00	1.1663	0.3136	0.21
07	0.99581	-0.55569	0.00	0.00	0.00	0.00
08	1.09	-0.55569	0.00	0.58285	0.00	0.00
09	0.94667	-0.59511	0.00	0.00	0.826	0.4648
10	0.94555	-0.61096	0.00	0.00	0.252	0.1624
11	0.99658	-0.60843	0.00	0.00	0.098	0.0504
12	1.0256	-0.61284	0.00	0.00	0.1708	0.0448
13	1.0205	-0.59129	0.00	0.00	0.378	0.1624
14	1.03	-0.45777	1.2	0.03683	0.4172	0.14

Table 4.11: Q-V model analysis result with SVC on bus 14

Eigenvalue number	Most Associated Bus	Eigenvalue (real part)	Eigenvalue (imaginary part)	Participation factor
1	04	62.2398	0.00	0.53022
2	02	50.1183	0.00	0.70374
3	09	36.2009	0.00	0.57755
4	06	30.0549	0.00	0.68698
5	07	22.7785	0.00	0.29251
6	14	1.39448	0.00	0.12566
7	07	18.88	0.00	0.18936
8	13	16.3581	0.00	0.37173
9	03	14.6471	0.00	0.67261
10	11	11.6145	0.00	0.3205
11	12	3.9202	0.00	0.26634
12	01	4.7695	0.00	0.1359
13	08	6.3802	0.00	0.5399
14	14	6.0669	0.00	0.54341

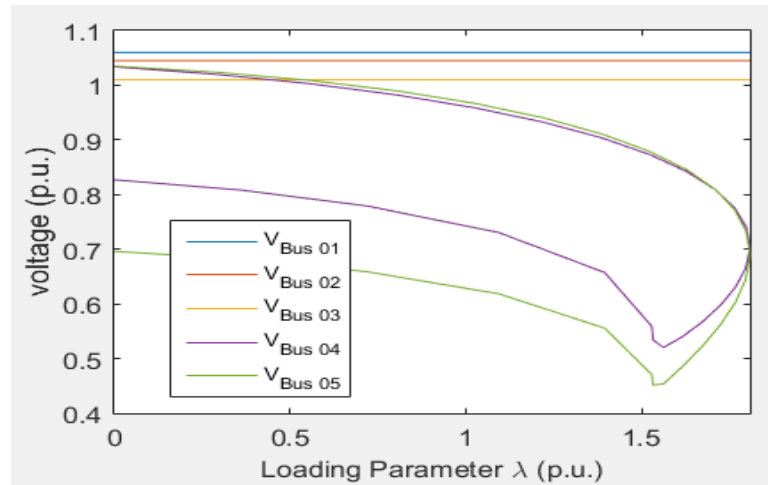


Figure 4.14: P-V curve after compensation for voltage at bus 1-bus 5

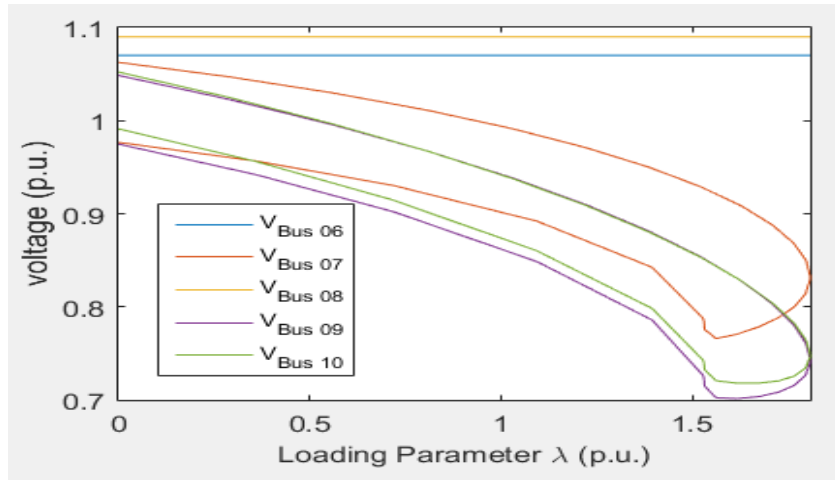


Figure 4.15: P-V curve after compensation for voltage at bus 6-bus 10

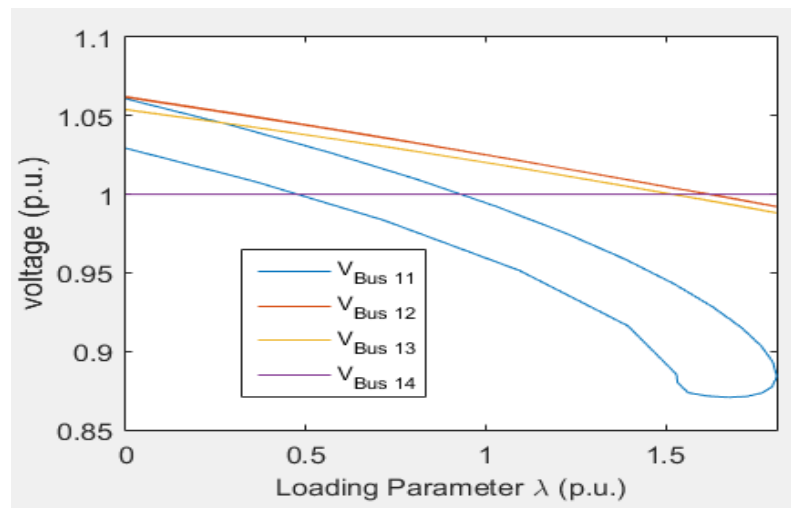


Figure 4.16: P-V curve after compensation for voltage at bus 11-bus 14

4.2.6 Voltage Stability Analysis for Power System with SVC at Bus 9 (Case 6)

A Static Var Compensator (SVC) device in this case is implemented on bus 9 which is case 6 of the study, voltage stability analysis for this case is shown below, where Table 4.12 shows the power flow result of the system after the implantation in bus 9, we can notice active and reactive power generation in bus 9 where it enhance the voltage magnitude for bus 9 to be 1.03 p.u. and the voltage magnitude of the other buses is improved. Table 4.13 shows the Eigenvalues of the system with participation factor for each bus, it's noticed the enhancement of the Q-V sensitivity values such as

increase in the eigenvalues making the system more stable. Figures (4.17), (4.18) and (4.19) show the P-V curve after the implementation SVC in bus 9, where the load parameter is increased reaching about 1.85 p.u. meaning that the system can handle more load increment before reaching to the collapse point which is the nose point of the curves as well as show that the buses maintain a high voltage magnitude after the collapse point when the high load release.

Table 4.12: Power flow result with SVC on bus 9

Bus number	Voltage (pu)	Angle (rad)	P generation (pu)	Q generation (pu)	P load (pu)	Q load (pu)
01	1.06	0.00	6.6935	-0.34528	0.00	0.00
02	1.045	-0.26904	0.4	2.5642	0.6076	0.3556
03	1.01	-0.65704	0.00	1.7833	2.6376	0.532
04	0.97018	-0.47722	0.00	0.00	1.3384	0.112
05	0.97242	-0.4095	0.00	0.00	0.2128	0.0448
06	1.07	-0.62797	0.00	1.0877	0.3136	0.21
07	1.0238	-0.52377	0.00	0.00	0.00	0.00
08	1.09	-0.52377	0.00	0.40976	0.00	0.00
09	1.03	-0.54806	1.2	0.2763	0.826	0.4648
10	0.99081	-0.57772	0.00	0.00	0.252	0.1624
11	1.0205	-0.60933	0.00	0.00	0.098	0.0504
12	1.0229	-0.66449	0.00	0.00	0.1708	0.0448
13	1.0079	-0.66038	0.00	0.00	0.378	0.1624
14	0.94611	-0.65333	0.00	0.00	0.4172	0.14

Table 4.13: Q-V model analysis result with SVC on bus 9

Eigenvalue number	Most Associated Bus	Eigenvalue (real part)	Eigenvalue (imaginary part)	Participation factor
1	04	62.7513	0.00	0.53375
2	02	50.1575	0.00	0.70387
3	09	37.8105	0.00	0.58614
4	06	30.0405	0.00	0.68856
5	07	23.1945	0.00	0.3322
6	14	1.29001	0.00	0.13411
7	07	19.1447	0.00	0.16528
8	13	16.2828	0.00	0.38952
9	03	14.6635	0.00	0.67521
10	11	11.8198	0.00	0.31621
11	12	3.9253	0.00	0.25794
12	01	4.9951	0.00	0.13078
13	08	6.4094	0.00	0.54055
14	14	5.9464	0.00	0.62411

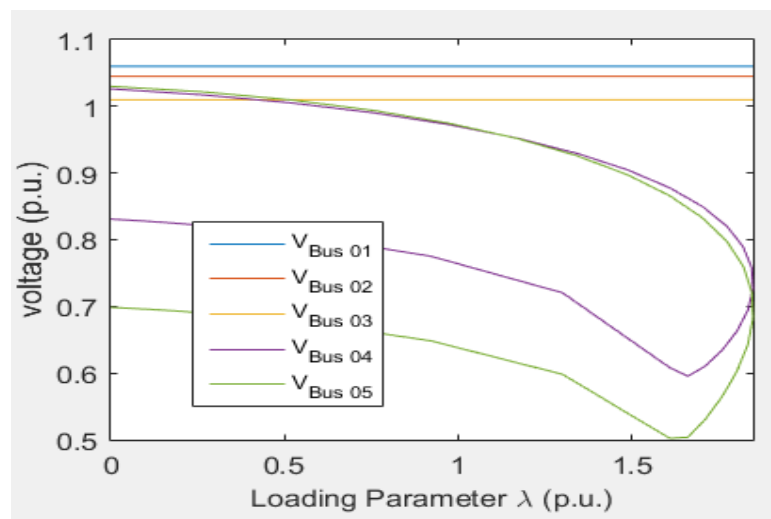


Figure 4.17: P-V curve after compensation for voltage at bus 1-bus 5

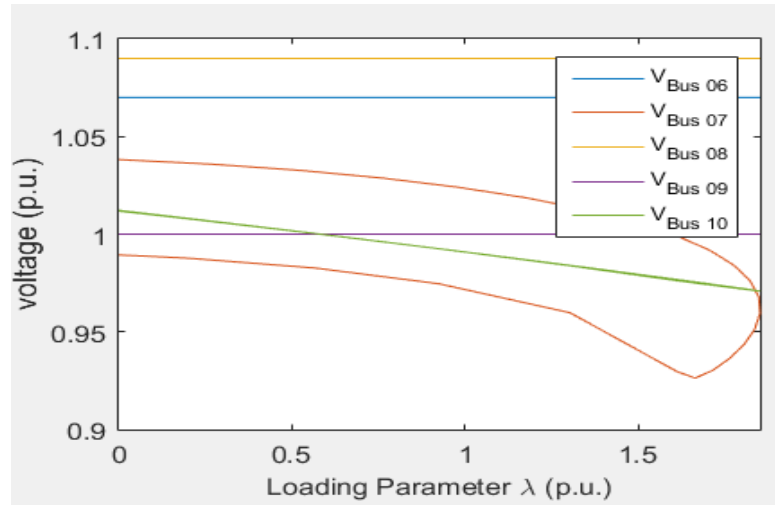


Figure 4.18: P-V curve after compensation for voltage at bus 6-bus 10

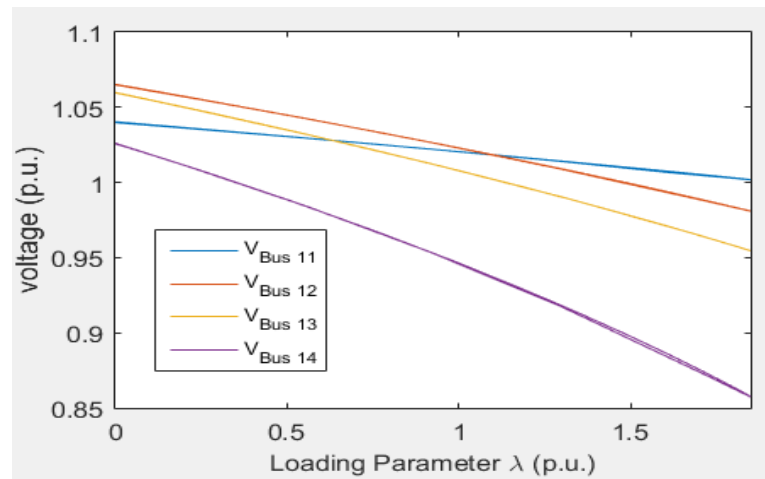


Figure 4.19: P-V curve after compensation for voltage at bus 11-bus 14

4.2.7 Voltage Stability Analysis for Power System with SVC at Bus 4 (Case 7)

A Static Var Compensator (SVC) device in this case is implemented on bus 4 which is case 7 of the study, voltage stability analysis for this case is shown below, where Table 4.14 shows the power flow result of the system after the implantation of SVC in bus 4, we can notice active and reactive power generation in bus 4 which enhance the voltage magnitude for bus 4 to be 1.03 p.u. and the voltage profile enhanced in the power system but because of the far distance between the bus 4 and the bus 14 and the power loss in the transmission system the voltage magnitude in the bus 14 still low as shown below in the power flow table. Table 4.15 shows the Eigenvalues of the system

with participation factor for each bus, results of the Q-V analysis shows that eigenvalues have been slightly increased which mean that the system stable and able to handle more load. Figures (4.20). (4.21) and (4.22) show the P-V curve after the implementation in bus 4, where the load parameter is increased reaching 2p.u. meaning that the system can handle more load increment before reaching to the collapse point which is the nose point of the curves, as well as returning the voltage magnitude to normal values after the nose point.

Table 4.14: Power flow result with SVC on bus 4

Bus number	Voltage (pu)	Angle (rad)	P generation (pu)	Q generation (pu)	P load (pu)	Q load (pu)
01	1.06	0.00	6.6673	-0.39897	0.00	0.00
02	1.045	-0.26566	0.4	2.2737	0.6076	0.3556
03	1.01	-0.64293	0.00	1.5868	2.6376	0.532
04	1.03	-0.47181	1.2	1.0567	1.3384	0.112
05	0.98578	-0.41473	0.00	0.00	0.2128	0.0448
06	1.07	-0.70856	0.00	1.1356	0.3136	0.21
07	1.0066	-0.63122	0.00	0.00	0.00	0.00
08	1.09	-0.63122	0.00	0.51638	0.00	0.00
09	0.95669	-0.72059	0.00	0.00	0.826	0.4648
10	0.9539	-0.73413	0.00	0.00	0.252	0.1624
11	1.0008	-0.72703	0.00	0.00	0.098	0.0504
12	1.0201	-0.75172	0.00	0.00	0.1708	0.0448
13	1	-0.75343	0.00	0.00	0.378	0.1624
14	0.91745	-0.79462	0.00	0.00	0.4172	0.14

Table 4.15: Q-V model analysis result with SVC on bus 4

Eigenvalue number	Most Associated Bus	Eigenvalue (real part)	Eigenvalue (imaginary part)	Participation factor
1	04	63.5615	0.00	0.53078
2	02	50.2242	0.00	0.70437
3	09	36.5239	0.00	0.57845
4	06	29.9017	0.00	0.68971
5	07	22.9144	0.00	0.30197
6	07	18.8581	0.00	0.18355
7	13	16.1288	0.00	0.38832
8	03	14.664	0.00	0.6572
9	14	1.0309	0.00	0.13036
10	11	11.6073	0.00	0.32844
11	12	3.6473	0.00	0.24758
12	01	3.908	0.00	0.11745
13	08	6.3524	0.00	0.54288
14	14	5.7754	0.00	0.61845

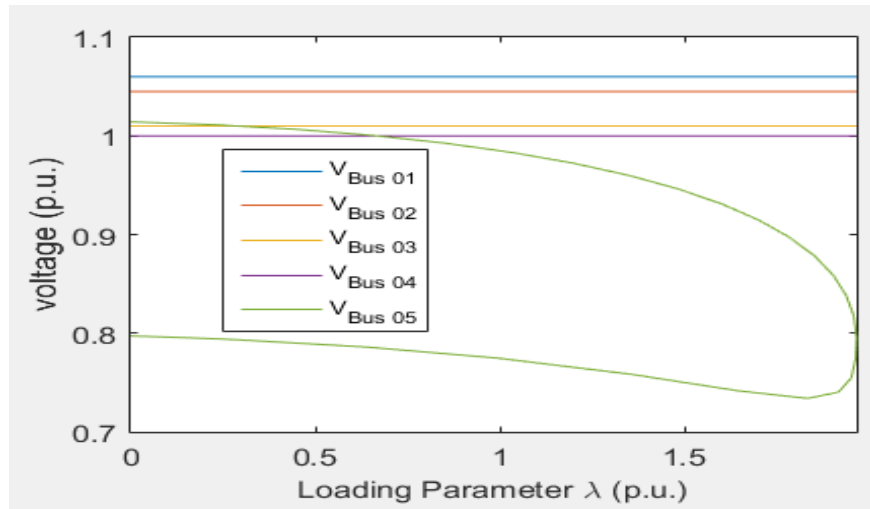


Figure 4.20: P-V curve after compensation for voltage at bus 1-bus 5

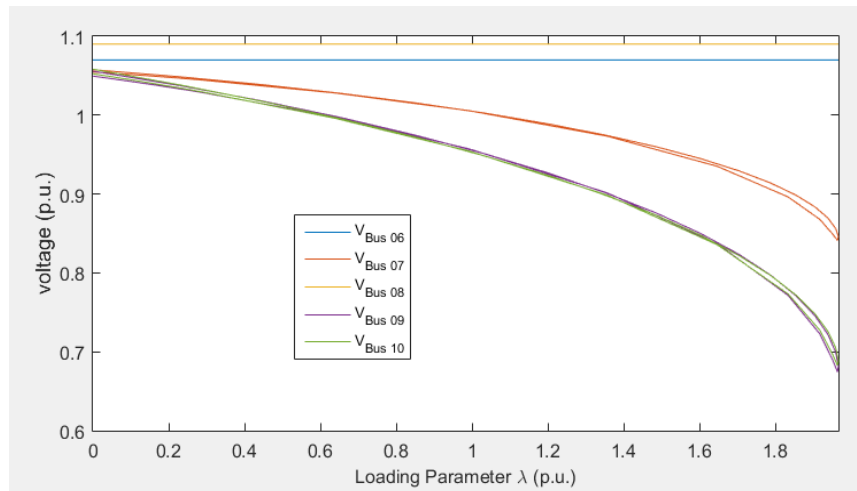


Figure 4.21: P-V curve after compensation for voltage at bus 6-bus 10

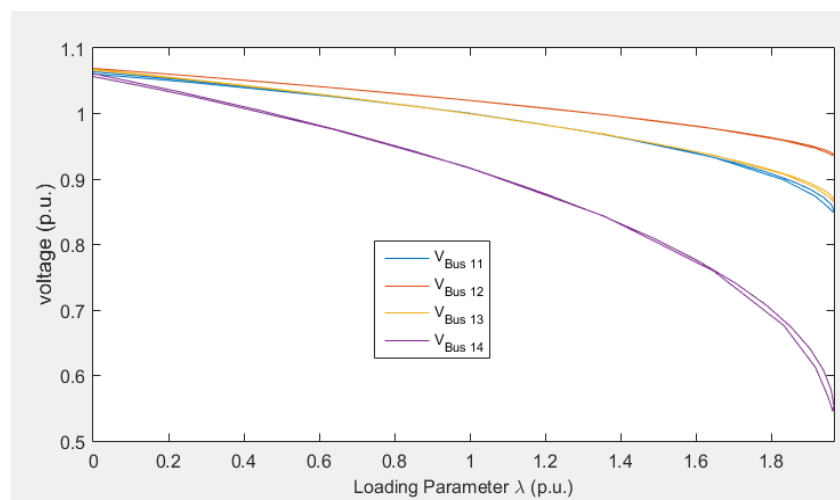


Figure 4.22: P-V curve after compensation for voltage at bus 11-bus 14

4.2.8 Voltage Stability Analysis for Power System with SVC at Bus 9 and STATCOM at Bus 14 (Case 8)

In this case the optimal locations have been found for the FACTS devices STATCOM and SVC to be implemented in the power system buses 14 and 9 respectively, the power flow study result is shown in table 4.16 below which shows that the voltage magnitude of the whole system is perfect as well as the active and reactive power generation from the buses 9 and 14 is noticed. Table 4.17 shows the Eigenvalues of the system with participation factor for each bus, the values of the eigenvalues have

been improved better than before making the system stability and load ability is the best between the all cases. Figures (4.23). (4.24) and (4.25) show the P-V curve after the implementation in bus the FACTS devices in bus 9 and bus 14, where the load parameter is increased reaching 2.3 p.u. which is the best load parameter and best system load ability among these cases which mean the system can handle more load than the other cases that have been discussed before.

Table 4.16: Power flow result with SVC on bus 9 and STATCOM on bus 14

Bus number	Voltage (pu)	Angle (rad)	P generation (pu)	Q generation (pu)	P load (pu)	Q load (pu)
01	1.06	0.00	4.8019	-0.44407	0.00	0.00
02	1.045	-0.19645	0.4	1.6733	0.6076	0.3556
03	1.01	-0.53472	0.00	1.5991	2.6376	0.532
04	1.0017	-0.32555	0.00	0.00	1.3384	0.112
05	1.0035	-0.27286	0.00	0.00	0.2128	0.0448
06	1.07	-0.34072	0.00	1.1305	0.3136	0.21
07	1.0302	-0.26279	0.00	0.00	0.00	0.00
08	1.09	-0.26279	0.00	0.37029	0.00	0.00
09	1.03	-0.22915	1.2	0.42477	0.826	0.4648
10	1.0256	-0.26459	0.00	0.00	0.252	0.1624
11	1.0202	-0.3093	0.00	0.00	0.098	0.0504
12	1.0494	-0.34383	0.00	0.00	0.1708	0.0448
13	1.0355	-0.30383	0.00	0.00	0.378	0.1624
14	1.03	-0.04817	1.6	0.31837	0.4172	0.14

Table 4.17: Q-V model analysis result with SVC on bus 9 and STATCOM on bus 14

Eigenvalue number	Most Associated Bus	Eigenvalue (real part)	Eigenvalue (imaginary part)	Participation factor
1	04	64.6934	0.00	0.53034
2	02	48.7428	0.00	0.68727
3	09	38.2533	0.00	0.59842
4	06	29.4763	0.00	0.66151
5	07	23.3171	0.00	0.33161
6	10	18.9327	0.00	0.16958
7	13	16.0859	0.00	0.34419
8	03	12.4048	0.00	0.6665
9	11	11.6436	0.00	0.30368
10	01	5.42088	0.00	0.11139
11	14	3.749	0.00	0.14047
12	08	4.3434	0.00	0.37526
13	14	6.361	0.00	0.32624
14	14	6.8194	0.00	0.35874

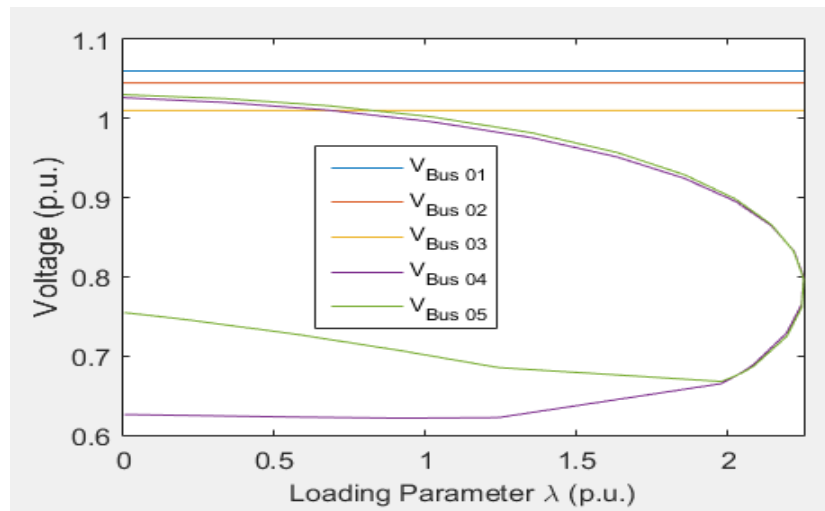


Figure 4.23: P-V curve after compensation for voltage at bus 1-bus 5

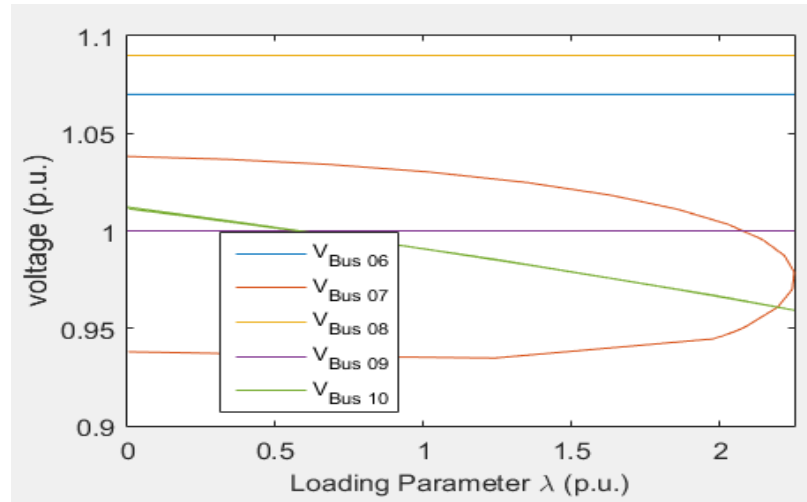


Figure 4.24: P-V curve after compensation for voltage at bus 6-bus 10

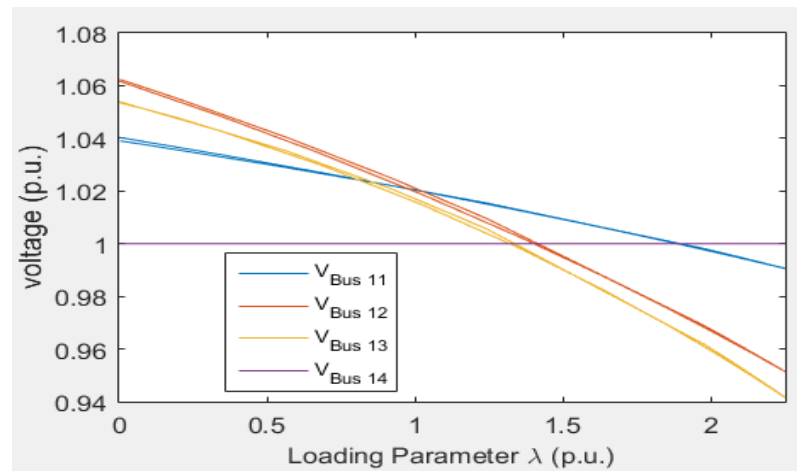


Figure 4.25: P-V curve after compensation for voltage at bus 11-bus 14

4.2.9 Dynamic Analysis of the System

Dynamic analysis is performed in the system where the voltage magnitude during time for each bus in the system is shown, Figure (4.26) shows the voltage magnitude for the first five buses of the system before adding the FACTS devices in the power system, this figure show how the voltage fluctuate during the operating time meaning the system is unreliable and unstable, followed with figures (4.27) and (4.28) for the voltage magnitudes of the rest buses.

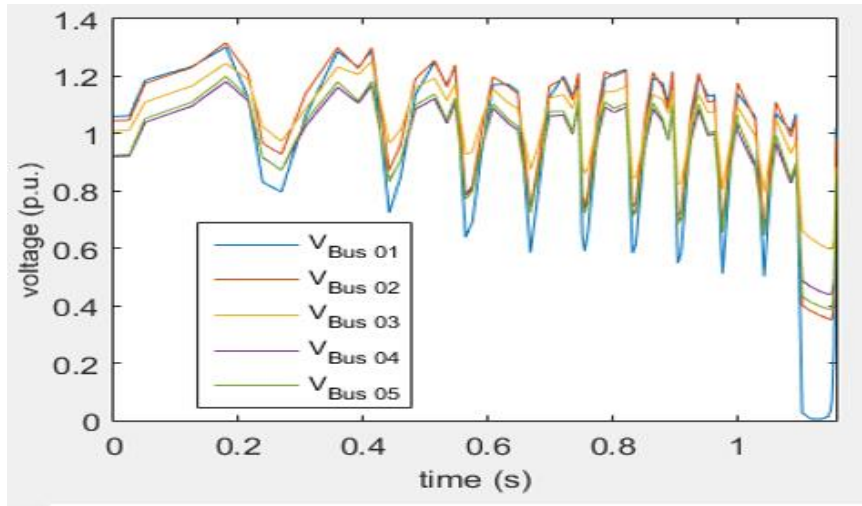


Figure 4.26: Time domain before compensation for voltage at bus 1-bus5

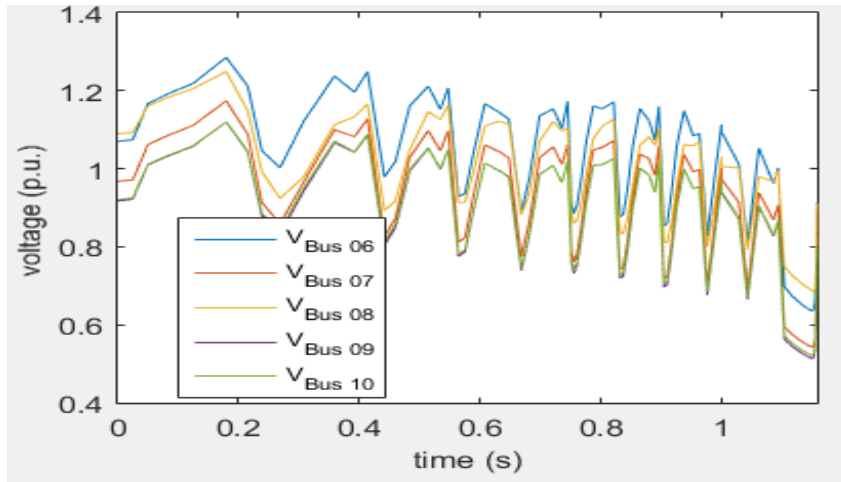


Figure 4.27: Time domain before compensation for voltage at bus 6-bus 10

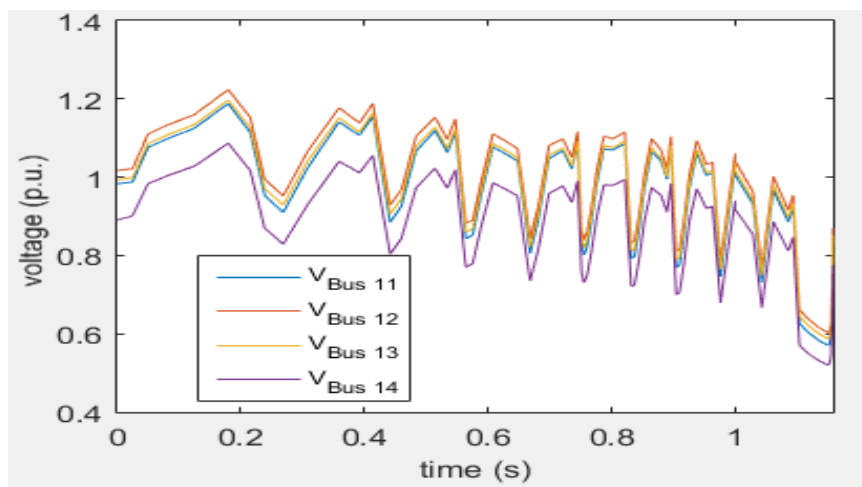


Figure 4.28: Time domain before compensation for voltage at bus 10-bus14

Dynamic analysis have been done as well for the optimal solution of this work which is case 8. Figure (4.29) shows the voltage magnitude for the first five buses in the system during time simulation about 30 seconds and it can easily be noticed how the power system voltage magnitude have way less fluctuation during time meaning that the system is stable during the operating time, followed with figures (4.30) and (4.31) for the voltage magnitudes of the rest buses.

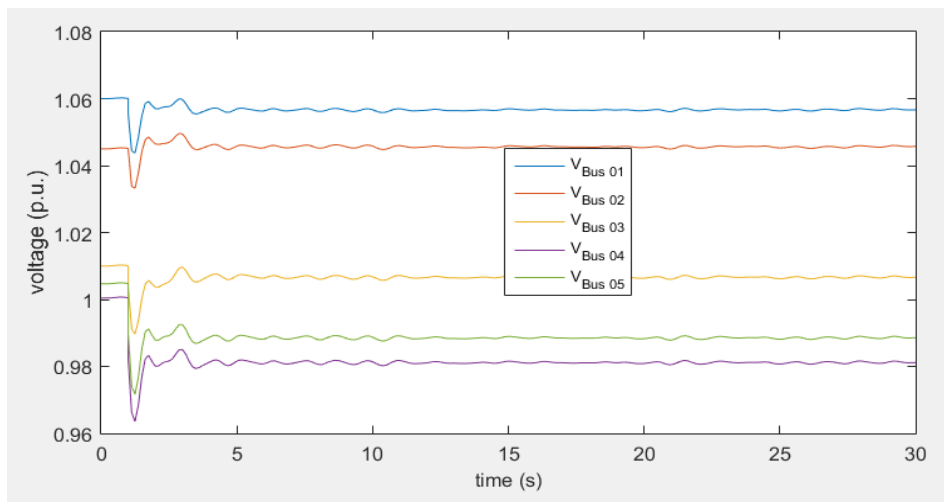


Figure 4.29: Time domain after compensation for voltage at bus 1-bus5

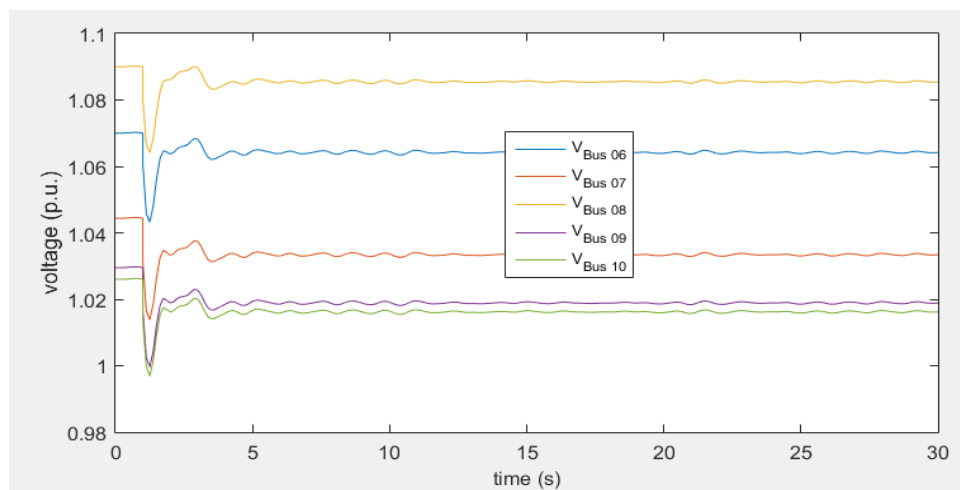


Figure 4.30: Time domain after compensation for voltage at bus 6-bus10

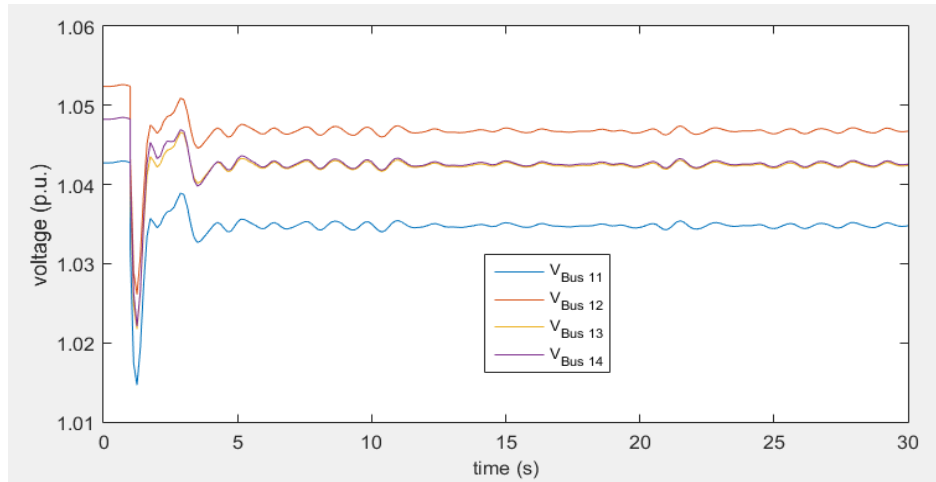


Figure 4.31: Time domain after compensation for voltage at bus 11-bus14

4.3 Comparison Between This Work and Past Works

As mentioned before in literature review the voltage stability analysis include static and dynamic analysis have been performed in many different power system in terms of power flow, Q-V sensitivity and P-V curves. Dynamic analysis of the past works was focusing in the FACTS devices performance and response time to contingency occur on the power system. In This work voltage stability analysis technique have been done on an IEEE-14 bus system where the static analysis included power flow, Q-V sensitivity as well as P-V curves, but in terms of dynamic analysis voltage magnitude fluctuation during time have been done and plotted.

Chapter 5

CONCLUSION

This thesis shows the importance of maintaining the power system voltage stable, if the voltage instability didn't get fixed in time it can lead the power system to collapse and blackout causing dark days in the power system. This thesis shows an overview and background of the voltage stability analysis and explanation of the different analysis techniques including power flow, P-V curve, and Q-V sensitivity in terms of the static part where the voltage magnitude during time simulation is the dynamic part. Voltage stability analysis and the use of different FACTS devices in different weakest areas in the power system have been done on the power system in order to improve the system stability. STATCOM and SVC model is explained as well as the wind farm model. Voltage stability analysis techniques are performed on IEEE-14 bus system in order to determine the weakest areas, as well as implement the FACTS devices in 8 different cases in order to enhance the power system and voltage profile. Dynamic analysis of the system showed the voltage fluctuation for each bus during time.

Voltage stability analysis for the system before the compensation shows the system is unstable and unreliable after adding FACTS devices in the two weakest buses in the system the voltage profile enhanced and the system is more stable and reliable, as well as show that the system can handle more increment in the load as well as show that the voltage magnitude fluctuation is more stable after the compensation. Moreover, it also

shows that the STATCOM device has more performance efficiency than the SVC device.

This thesis targets the electrical and electronic engineer who works in power systems where it provides a systematic approach to analyze the system stability and perform FACTS devices using the software PSAT. The FACTS devices can be sized after the implantation in the power system where the prices of these devices increase exponentially with the size of it, as well as there is many different FACTS devices such as Static Synchronous Series Compensator (SSSC) that can be used and tested in the system in order to enhance the power system stability.

REFERENCES

- [1] R. M, "The optimisation of stand-alone hybrid renewable energy systems using homer," *International Review of Electrical Engineering*, 2011.

- [2] T. R. Ayodele, "Challenges of grid integration of wind power on power system grid integrity: a review," *International Journal of Renewable Energy Research (IJRER)*, pp. 618-626, 2012.

- [3] P. K. "Definition and classification of power system stability IEEE/CIGRE joint task force on stability terms and definitions.," *Power Systems, IEEE Transactions on*, pp. 1387-1401, 2004.

- [4] N. Acharya, A. Sode-Yome and N. Mithulananthan, "Facts about flexible AC transmission systems (FACTS) controllers: practical installations and benefits".

- [5] B. B. Adetokun, C. M. Muriithi and J. O. Ojo, "Voltage stability assessment and enhancement of power grid with increasing wind energy penetration," *Electrical Power and Energy Systems*, 2020.

- [6] S. R. Inkollu and V. . R. Kota, "Optimal setting of FACTS devices for voltage stability improvement using PSO adaptive GSA hybrid algorithm," *Engineering Science and Technology,an International Journal*, pp. 1166-1176, 2016.

- [7] S. d. Nascimento and M. M. Gouvêa Jr, "Voltage stability enhancement in power systems with automatic facts device allocation," *Energy Procedia*, pp. 60-67, 2017.
- [8] S. Gasperic and R. Mihalic, "Estimation of the efficiency of FACTS devices for voltage-stability enhancement with PV area criteria," *Renewable and Sustainable Energy Reviews*, pp. 144-156, 2019.
- [9] P. Prabhakar and A. Kumar, "Voltage stability boundary and margin enhancement with FACTS and HVDC," *Electrical Power and Energy Systems*, pp. 429-438, 2016.
- [10] S. Gasperic and R. Mihalic, "The impact of serial controllable FACTS devices on voltage stability," *Electrical Power and Energy Systems*, pp. 1040-1048, 2015.
- [11] P. Sharma and A. Kumar, "Thevenin's equivalent based P-Q-V voltage stability region visualization and enhancement with FACTS and HVDC," *Electrical Power and Energy Systems*, pp. 119-127, 2016.
- [12] S. R. Inkollu and V. R. Kota, "Optimal setting of FACTS devices for voltage stability improvement using PSO adaptive GSA hybrid algorithm," *Engineering Science and Technology, an International Journal*, pp. 1166-1176, 2016.

- [13] A. S. Saidi, "Impact of grid-tied photovoltaic systems on voltage stability of tunisian distribution networks using dynamic reactive power control," *Ain Shams Engineering Journal*, 2022.
- [14] A. A. Nafeh, A. Heikal, R. A. El-Sehiemy and W. A. Salem, "Intelligent fuzzy-based controllers for voltage stability enhancement of AC-DC micro-grid with D-STATCOM," *Alexandria Engineering Journal*, pp. 2260-2293, 2022.
- [15] S. P. Jaiswal, V. Shrivastava and D. K. Palwalia, "Impact of semiconductor devices on voltage stability of distribution system," *Materials Today: Proceedings*, pp. 581-589, 2019.
- [16] S. Ranjan, A. Latif, D. C. Das, N. Sinha, S. . S. Hussain, T. S. Ustun and A. Iqbal, "Simultaneous analysis of frequency and voltage control of the interconnected hybrid power system in presence of FACTS devices and demand response scheme," *Energy Reports*, pp. 7445-7459, 2021.
- [17] B. Bhattacharyya and S. Raj, "Swarm intelligence based algorithms for reactive power planning with Flexible AC transmission system devices," *Electrical Power and Energy Systems*, pp. 158-164, 2016.
- [18] R. Sakipour and H. Abdi, "Voltage stability improvement of wind farms by self-correcting static volt-ampere reactive compensator and energy storage," *International Journal of Electrical Power & Energy Systems*, 2022.

- [19] P. He, Q. Fang, H. Jin, Y. Ji, Z. Gong and J. Dong, "Coordinated design of PSS and STATCOM-POD based on the GA-PSO algorithm to improve the stability of wind-PV-thermal-bundled power system," *International Journal of Electrical Power & Energy Systems*, 2022.
- [20] C. Li, R. Burgos, B. Wen, Y. Tang and D. Boroyevich, "Stability analysis of power systems with multiple STATCOMs in close proximity," *IEEE Transactions on Power Electronics*, pp. 2268-2283, 2019.
- [21] S. Yu, T. Fernando, T. K. Chau and H. H.-C. Iu, "Voltage control strategies for solid oxide fuel cell energy system connected to complex power grids using dynamic state estimation and STATCOM," *IEEE Transactions on Power Systems*, pp. 3136-3145, 2016.
- [22] L. Wang, C.-H. Chang, B.-L. Kuan and A. V. Prokhorov, "Stability improvement of a two-area power system connected with an integrated onshore and offshore wind farm using a STATCOM," *IEEE Transactions on Industry Applications*, pp. 867-877, 2016.
- [23] G. S. Chawda, A. G. Shaik, O. P. Mahela, S. Padmanaban and J. B. Holm-nielsen, "Comprehensive review of distributed FACTS control algorithms for power quality enhancement in utility grid with renewable energy penetration," *IEEE Access*, pp. 107614-107634, 2020.

- [24] S. Yu, T. K. Chau, T. Fernando, A. V. Savkin and H. H.-C. Iu, "Novel quasi-decentralized SMC-based frequency and voltage stability enhancement strategies using valve position control and FACTS device," *IEEE Access*, pp. 946-955, 2016.
- [25] Y. Terriche, C.-L. Su, A. Lashab, M. U. Mutarraf, M. Mehrzadi, J. M. Guerrero and J. C. Vasquez,, "Design of cost-effective compensators to enhance voltage stability and harmonics contamination of high-power more electric marine vessels," *IEEE Transactions on Industry Applications*, pp. 4130-4142, 2021.
- [26] M. A. Kamarposhti, H. Shokouhandeh, I. Colak, S. S. Band and K. Eguchi, "Optimal location of FACTS devices in order to simultaneously improving transmission losses and stability margin using artificial bee colony algorithm," *IEEE Access*, pp. 125920-125929, 2021.
- [27] F. Aydin and B. Gumus, "Determining optimal SVC location for voltage stability using multi-criteria decision making based solution: analytic hierarchy process (AHP) approach," *IEEE Access*, pp. 143166-143180, 2021.
- [28] S. Shukla and L. Mili, "Hierarchical decentralized control for enhanced rotor angle and voltage stability of large-scale power systems," *IEEE Transactions on Power Systems*, pp. 4783-4793, 2017.

- [29] H. Nazaripouya and S. Mehraeen, "Modeling and nonlinear optimal control of weak/islanded grids using FACTS device in a game theoretic approach," *IEEE Transactions on Control Systems Technology*, pp. 158-171, 2015.
- [30] G. Pierrou and X. Wang, "An online network model-free wide-area voltage control method using PMUs," *IEEE Transactions on Power Systems*, pp. 4672 - 4682, 2021.
- [31] Y. Wan, M. A. A. Murad, M. Liu and F. Milano, "Voltage frequency control using SVC devices coupled with voltage dependent loads," *IEEE Transactions on Power Systems*, pp. 1589 - 1597, 2018.
- [32] S. Nascimento, R. M. Batalha and M. M. Gouvêa Jr., "Adaptive evolutionary algorithm applied to the voltage stability problem in power systems," *IEEE Access*, pp. 69149 - 69161, 2018.
- [33] G. I. Rashed, H. Haider and M. Shafik, "Enhancing energy utilization efficiency of Pakistani system considering FACTS devices and distributed generation: feasibility study," *Chinese Journal of Electrical Engineering*, pp. 66 - 82, 2020.
- [34] B. Saleem, R. Badar, A. Manzoor, M. A. Judge, J. Boudjadar and S. U. Islam, "Fully adaptive recurrent neuro-fuzzy control for power system stability enhancement in multi machine system," *IEEE Access*, pp. 36464 - 36476, 2022.

- [35] B. Ismail, N. I. Abd Wahab, M. L. Othman, M. A. Mohd Radzi, K. . N. Vijyakumar and M. M. Naain, "A comprehensive review on optimal location and sizing of reactive power compensation using hybrid-based approaches for power loss reduction, voltage stability improvement, voltage profile enhancement and loadability enhancement," *IEEE Access*, pp. 222733 - 222765, 2020.
- [36] A. M. Eltamaly, Y. Sayed, A.-H. M. El-sayed and A. N. A. Elghaffar, "Optimum power flow analysis by newton raphson method, a case study," *ANNALS of Faculty Engineering Hunedoara – International Journal of Engineering*, 2019.
- [37] R. Sirjani and N. T. Bolan, "An improved cuckoo search algorithm for voltage stability enhancement in power transmission networks," *International Journal of Energy and Power Engineering*, 2016.
- [38] V. Ajjarapu, "Computational techniques for voltage stability assessment and control," in *Power Electronics and Power Systems*, Boston, Springer, 2006, p. 49–116.
- [39] S. H. Hosseinian, "Improvements in power system transient simulation by application of trigonometric trapezoidal rule," *Computer Applications in Engineering Education*, pp. 277-289, 2008.

[40] R. Sirjani, A. Mohamed and H. Shareef, "Comparative study of effectiveness of different var compensation devices in large scale power networks," *journal of Central South University of Technology*, 2013.

[41] K. Z. Heetun, S. H. Abdel Aleem and A. F. Zobaa, "Voltage stability analysis of grid-connected wind farms with FACTS: static and dynamic analysis," *Energy and Policy Research*, pp. 1-12, 2016.